

SOLVING A CLASS OF INFINITE-DIMENSIONAL TENSOR EIGENVALUE PROBLEMS BY TRANSLATIONAL INVARIANT TENSOR RING APPROXIMATIONS*

ROEL VAN BEEUMEN[†], LANA PERIŠA[‡], DANIEL KRESSNER[§], AND CHAO YANG[†]

Abstract. We examine a method for solving an infinite-dimensional tensor eigenvalue problem $Hx = \lambda x$, where the infinite-dimensional symmetric matrix H exhibits a translational invariant structure. We provide a formulation of this type of problem from a numerical linear algebra point of view and describe how a power method applied to e^{-Ht} is used to obtain an approximation to the desired eigenvector. This infinite-dimensional eigenvector is represented in a compact way by a translational invariant infinite Tensor Ring (iTR). Low rank approximation is used to keep the cost of subsequent power iterations bounded while preserving the iTR structure of the approximate eigenvector. We show how the averaged Rayleigh quotient of an iTR eigenvector approximation can be efficiently computed and introduce a projected residual to monitor its convergence. In the numerical examples, we illustrate that the norm of this projected iTR residual can also be used to automatically modify the time step t to ensure accurate and rapid convergence of the power method.

Key words. infinite eigenvalue problem, tensor eigenvalue problem, tensor ring, tensor train, translational invariance, matrix product states

AMS subject classifications. 15A18, 15A21, 15A69, 65F15

1. Introduction. To motivate the infinite-dimensional eigenvalue problems considered in this work, we will first consider the finite-dimensional eigenvalue problem $\mathcal{H}_\ell x_\ell = \lambda^{(\ell)} x_\ell$, where the symmetric matrix $\mathcal{H}_\ell \in \mathbb{R}^{d^{2\ell+1} \times d^{2\ell+1}}$ is defined as the following sum of Kronecker products

$$(1.1) \quad \mathcal{H}_\ell = \sum_{k=-\ell}^{\ell-1} \tilde{H}_k, \quad \tilde{H}_k = I \otimes \cdots \otimes I \otimes M_{k,k+1} \otimes I \otimes \cdots \otimes I,$$

with the $d \times d$ identity matrix I and $M_{k,k+1} \in \mathbb{R}^{d^2 \times d^2}$. We will assume that the matrices $M_{k,k+1}$ are the same for every k ; the subscript $k, k+1$ is used to merely indicate the overlapping positions of M in each Kronecker product. Note that x_ℓ can equivalently be viewed as a $d \times \cdots \times d$ tensor of order $2\ell+1$. This type of tensor eigenvalue problems originates from the study of model quantum many-body systems such as a quantum spin chain with nearest neighbor interactions [4]. The Kronecker structure of \mathcal{H}_ℓ allows for efficiently representing such matrices and their eigenvectors in, e.g., the Tensor Train (TT) format [15]. The TT format of an eigenvector takes the form

$$(1.2) \quad x_\ell(i_{-\ell}, i_{-\ell+1}, \dots, i_{\ell-1}, i_\ell) = X_{-\ell}(i_{-\ell})X_{-\ell+1}(i_{-\ell+1}) \cdots X_{\ell-1}(i_{\ell-1})X_\ell(i_\ell),$$

where $i_k = 1, \dots, d$, with $k = -\ell, \dots, \ell$, and each $X_k(i_k)$ is an $r_k \times r_{k+1}$ matrix, with $r_{-\ell} = r_{\ell+1} = 1$.

*Submitted to the editors October 4, 2023.

Funding: This work was partially funded by the U.S. Department of Energy, Office of Science, Office of Advanced Scientific Computing Research, Scientific Discovery through Advanced Computing (SciDAC) program under Contract No. DE-AC0205CH11231.

[†]Applied Mathematics and Computational Research Division, Lawrence Berkeley National Laboratory, Berkeley, CA 94720, United States. (rvanbeeumen@lbl.gov, cyang@lbl.gov).

[‡]Visage Technologies, Diskettgatan 11A, SE-583 35 Linköping, Sweden. (ana.perisa@visagetechnologies.com).

[§]Department of Mathematics, École Polytechnique Fédérale de Lausanne, Station 8, 1015 Lausanne, Switzerland. (daniel.kressner@epfl.ch).

In this paper, we consider \mathcal{H}_ℓ as $\ell \rightarrow \infty$. Such limits are known in the physics literature as the *thermodynamic limit* and they are important for describing macroscopic properties of quantum materials [19]. Taking $\ell \rightarrow \infty$ in (1.1) *formally* leads to the following infinite-dimensional symmetric matrix

$$(1.3) \quad \mathbf{H} = \sum_{k=-\infty}^{+\infty} \mathbf{H}_k, \quad \mathbf{H}_k = \cdots \otimes I \otimes I \otimes M_{k,k+1} \otimes I \otimes I \otimes \cdots,$$

where, again, all matrices $M_{k,k+1}$ are identical and, hence, \mathbf{H} is called *translational invariant*. It is important to emphasize that we make no attempt to mathematically frame or justify convergence of the formal series (1.3). In fact, even the eigenvalues of (1.3) are usually infinite in the sense that the eigenvalues of the matrix \mathcal{H}_ℓ defined in (1.1) become unbounded as ℓ grows. To avoid this, one considers averaged eigenvalues of the form $\lambda^{(\ell)}/(2\ell)$, where $\lambda^{(\ell)}$ is an eigenvalue of \mathcal{H}_ℓ . We are particularly interested in the smallest among these averaged eigenvalues as $\ell \rightarrow \infty$. This is referred to in the physics literature as the ground state energy per site [1, 23]. For some specific choices of M , the analytical solutions of these eigenvalue problems are known [3, 10, 2]. However, in general, the desired averaged eigenvalue and its corresponding eigenvector need to be computed numerically. One way to study such an infinite problem computationally is to start with a finite value of ℓ and examine how the smallest averaged eigenvalue changes as ℓ increases. However, applying a standard eigensolver to \mathcal{H}_ℓ severely limits the feasible range of ℓ even on a powerful supercomputer, and one may not attain a reasonably good approximation to the limit $\ell \rightarrow \infty$. It is therefore preferable to directly work with the \mathbf{H} from (1.3). Due to the infinite dimensionality, special care must be exercised when computing quantities such as the Rayleigh quotient and the residual of an approximate eigenpair of \mathbf{H} .

As the eigenvectors of \mathbf{H} are infinite-dimensional vectors, they obviously cannot be computed or stored directly in memory. On the other hand, we can represent them in a compact form by making use of the translational invariance property of \mathbf{H} . Such an invariance property was studied by Bethe [3] and Hulthén [10], known as the *Bethe–Hulthén hypothesis*, which imposes that the elements of the eigenvector are invariant with respect to a cyclic permutation of the tensor indices, i.e., $\mathbf{x}(\dots, i_{-1}, i_0, i_1, \dots) = \mathbf{x}(\dots, i_0, i_1, i_2, \dots)$, where $i_k = 1, \dots, d$, and the sequence of indices $\dots, i_{-1}, i_0, i_1, \dots$ specifies a particular element of the infinite-dimensional vector \mathbf{x} . We (approximately) represent the eigenvector to be computed as a translational invariant *infinite Tensor Ring* (iTR), defined as

$$\mathbf{x}(\dots, i_{-1}, i_0, i_1, \dots) = \text{Tr} \left[\prod_{k=-\infty}^{+\infty} X(i_k) \right],$$

where $i_k = 1, \dots, d$ for every k and each $X(i_k)$ is an $r \times r$ matrix. Note that, thanks to the translational invariance, this allows us to store and work with d matrices of size $r \times r$, which is manageable as long as the rank r is not too large. An iTR can be seen as the infinite limit of a finite size tensor ring [25] and is also known as a uniform Matrix Product State (uMPS) [24].

We assume that the averaged eigenvalue of interest is simple and propose to apply a power iteration to $e^{-\mathbf{H}t}$ for some small and adjustable parameter $t > 0$ to compute the desired eigenpair. We should note that the power method is not the only method for solving this type of infinite-dimensional tensor eigenvalue problems. Alternative methods include the infinite density matrix renormalization (iDMRG) method [22]

and the variational uniform matrix product states (vUMPS) method [24]. The main purpose of our paper is to formulate this type of problem from a numerical linear algebra point of view and describe how a standard numerical algorithm such as the power method can be modified and applied to address such problems.

In order to implement the power method, we must be able to multiply a matrix exponential with an iTR and keep the product in iTR form. Computing $e^{-\mathbf{H}t}\mathbf{x}$, with \mathbf{H} being an infinite-dimensional matrix and \mathbf{x} an iTR, is in general not possible. However, the special structure of (1.3) allows us to split \mathbf{H} in even and odd terms, \mathbf{H}_e and \mathbf{H}_o , respectively. For sufficiently small t , we can use the Lie product formula, also known as Suzuki–Trotter splitting, to approximate $e^{-\mathbf{H}t}\mathbf{x}$ by only local tensor contractions with a $d^2 \times d^2$ matrix exponential e^{-Mt} . Such contractions can be implemented in a way that the translational invariance of the contracted tensor is preserved, although the rank generally increases. To keep the cost of subsequent power iterations bounded, a low-rank approximation through the use of a truncated singular value decomposition is applied.

We should note that the approach described above was first developed in the physics community and called the infinite time evolution block decimation (iTEBD) method [21]. We prefer to refer to this approach as a *flexible* power method to clearly articulate the mathematical and algorithmic features of this numerical method. The use of the term “flexible” highlights the ability of the method to work with approximations of the matrix exponential $e^{-\mathbf{H}t}$. In the physics literature, the accuracy of the approximate eigenvalue is assessed by either comparing the approximation with the exact solution or examining the difference between the approximate eigenvalues obtained from two consecutive iterations. The former is not practical when the exact solution of the problem is unknown. The latter can be misleading when the power iteration starts to stagnate, which does happen as shown in our numerical experiments. Instead, we will show that the norm of a suitably defined residual can be used to monitor convergence. We give a practical procedure for adjusting the parameter t in the flexible power iteration to ensure rapid and stable convergence and provide a stopping criterion for terminating the power iteration. As illustrated in the numerical experiments, such a procedure is effective.

The rest of this paper is organized as follows. In section 2, we introduce diagrammatic notations for scalars, vectors, matrices, and tensors, as well as for tensor operations. These notations make it easier to explain operations performed on tensor rings. In section 3, we begin with a formal definition of a single core translational invariant infinite Tensor Ring, describe its properties, and show how an iTR can be converted into a so-called canonical form. We also extend these definitions and properties to 2-core translational invariant iTRs which are used to represent the approximate eigenvector of \mathbf{H} containing nearest neighbor interactions as in (1.3). In section 4, we define suitable notions of Rayleigh quotient and residual, and show how they can be evaluated efficiently with respect to an iTR. In section 5, we present the power iteration for computing the smallest eigenpair of \mathbf{H} . We also show how $e^{\mathbf{H}t}\mathbf{x}$ is computed to preserve the iTR structure and discuss a number of practical computational considerations regarding the convergence and error assessment of the method. Three numerical examples are given in section 6 to demonstrate the effectiveness of the power method and the adaptive strategy proposed in section 5. Finally, the main conclusions are summarized in section 7.

2. Notation. Throughout the paper, we denote scalars by lower case Greek characters, vectors by lower case Roman characters, and matrices and higher order

tensors by upper case Roman characters, e.g., α , x , and M , respectively. I_d is the $d \times d$ identity matrix and diagonal matrices are denoted by upper case Greek characters, e.g., Σ . The trace of a matrix M is given by $\text{Tr}(M)$ and its vectorization by $\text{vec}(M)$. For infinite-dimensional vectors and matrices we use boldface Roman characters, e.g., \mathbf{v} and \mathbf{M} , respectively.

We will make use of the powerful tensor diagram notation [16] to graphically represent tensor contractions. The first 4 low-order tensors, i.e., a scalar α , a vector v , a matrix M , and a 3rd-order tensor T , are depicted as follows

$$\alpha = \textcircled{\alpha}, \quad v = \overset{i}{\textcircled{v}}, \quad M = \overset{i}{\textcircled{M}} \overset{j}{\textcircled{M}}, \quad T = \overset{i}{\textcircled{T}} \overset{j}{\textcircled{T}} \underset{k}{\textcircled{T}}$$

where i, j, k are the corresponding tensor indices. In this graphical notation, tensor contractions can be represented by connecting the matching lines that correspond to the indices to sum over. For example, the matrix-vector product, the matrix-matrix product, and the contraction of two 3rd-order tensors into a so called *supercore* are given respectively by the following diagrams

$$Mv = \overset{i}{\textcircled{M}} \overset{j}{\textcircled{v}}, \quad MN = \overset{i}{\textcircled{M}} \overset{j}{\textcircled{N}} \overset{k}{\textcircled{N}}, \quad \overset{i}{\textcircled{Z}} \overset{j}{\textcircled{X}} \overset{k}{\textcircled{Y}} \overset{l}{\textcircled{Z}} = \overset{i}{\textcircled{X}} \overset{j}{\textcircled{Y}} \overset{k}{\textcircled{Z}} \overset{l}{\textcircled{Z}}$$

where the connections between M and v , M and N , and X and Y correspond to the sum over index j . Note that the thick leg indicates combining the indices k and l into a single index. Because contracting a tensor over one of its indices with the identity matrix has no effect, we represent the identity matrix I by just a line.

Some other commonly used matrix operations such as the trace, the transpose, and the vectorizations of a matrix are given by the following diagrams

$$\text{Tr}(M) = \textcircled{M}, \quad v^\top = \textcircled{v}, \quad \text{vec}(M) = \textcircled{M}, \quad \text{vec}(M)^\top = \textcircled{M}$$

In order to save space, we sometimes rotate the diagrams counterclockwise by 90 degrees. Throughout the paper, reshaping tensors into matrices and vice versa will play a key role, e.g., reshaping the following rank-1 matrices into 4th-order tensors

$$\text{vec}(I) \text{vec}(\Sigma^2)^\top = \left. \begin{array}{c} \textcircled{\Sigma} \\ \textcircled{\Sigma} \end{array} \right\}, \quad \text{vec}(\Sigma^2) \text{vec}(I)^\top = \left. \begin{array}{c} \textcircled{\Sigma} \\ \textcircled{\Sigma} \end{array} \right\}$$

where Σ is a diagonal matrix. We again obtain a matrix by combining respectively the left and right pointing legs into one index.

3. Translational invariant infinite tensor ring. In this section, we define a translational invariant infinite tensor ring and discuss its properties that will be used in the next sections to construct an approximation to the eigenvector associated with the smallest eigenvalue of the infinite-dimensional matrix \mathbf{H} defined by (1.3). We start by defining translational invariance for a (finite) tensor ring.

3.1. Finite tensor ring. The tensor ring decomposition [11, 25, 13] is a way to represent high-order tensors (or vectors that can be reshaped into high-order tensors) by a sequence of 3rd-order tensors multiplied in circular fashion.

DEFINITION 3.1 (Tensor ring). *Let x_ℓ be an ℓ th-order tensor of size $d_1 \times d_2 \times \dots \times d_\ell$. We say that x_ℓ is in tensor ring representation if there exist 3rd-order tensors X_k ,*

$k = 1, 2, \dots, \ell$ of sizes $r_k \times d_k \times r_{k+1}$, with $r_{k+1} = r_1$, such that x_ℓ can be represented element-wise as $x_\ell(i_1, i_2, \dots, i_\ell) = \text{Tr}(X_1(i_1)X_2(i_2) \cdots X_\ell(i_\ell))$ for $i_k \in \{1, 2, \dots, d_k\}$, where $X_k(i_k)$ denotes the i_k th lateral slice of X_k . The integers r_1, r_2, \dots, r_ℓ are called tensor ring ranks. Graphically, a tensor ring representation corresponds to

$$x_\ell = \overbrace{\left(\begin{array}{c} \boxed{X_1} - \boxed{X_2} - \cdots - \boxed{X_\ell} \\ | \quad | \quad \quad | \\ i_1 \quad i_2 \quad \quad i_\ell \end{array} \right)}.$$

The 3rd-order tensors X_k are called the *cores* of x_ℓ , with $X_k(i_k)$ being the *slice* of the k th core. In the physics literature, a tensor ring is called a matrix product state with periodic boundary conditions [17]. When $r_1 = r_{\ell+1} = 1$, a tensor ring becomes a *tensor train* (1.2), also known in the physics literature as a matrix product state with open boundary conditions [17].

When $d_k = d$, $r_k = r$, and $X_k(i_k) \equiv X(i_k)$ for every $k = 1, 2, \dots, \ell$, the tensor ring x_ℓ is said to be translational invariant. In this case, the cyclic property of the trace implies

$$x_\ell(i_1, i_2, \dots, i_\ell) = x_\ell(i_2, \dots, i_\ell, i_1),$$

that is, x_ℓ is invariant under cyclic permutations of its indices. This is a desirable property because the eigenvectors of \mathbf{H} defined in (1.3) are known to have such a property for certain $M_{k,k+1}$. We define a translational invariant (finite) tensor ring as follows.

DEFINITION 3.2 (Translational invariant TR). *Let X be an $r \times d \times r$ tensor. We define a translational invariant (finite) tensor ring element-wise as $x_\ell(i_1, i_2, \dots, i_\ell) := \text{Tr}[X(i_1)X(i_2) \cdots X(i_\ell)]$ for $i_k \in \{1, 2, \dots, d\}$. We refer to r as the (tensor ring) rank of x_ℓ . Graphically, this representation corresponds to*

$$x_\ell = \overbrace{\left(\begin{array}{c} \boxed{X} - \boxed{X} - \cdots - \boxed{X} \\ | \quad | \quad \quad | \\ i_1 \quad i_2 \quad \quad i_\ell \end{array} \right)}.$$

Note that, due to the translational invariance, storing the tensor ring x_ℓ only requires to store a single core X of size $r \times d \times r$.

3.2. Infinite tensor ring. Practically, it is difficult to generalize Definition 3.1 to tensor rings with an infinite number of cores because this would require an infinite amount of data to represent \mathbf{x} . In contrast, it is possible to generalize Definition 3.2 to infinite tensor rings (iTR).

DEFINITION 3.3 (Translational invariant iTR). *Let X be an $r \times d \times r$ tensor. We define a translational invariant infinite tensor ring element-wise as*

$$x(\dots, i_{-1}, i_0, i_1, \dots) = \lim_{\ell \rightarrow \infty} \text{Tr} \left(\prod_{k=-\ell}^{\ell} X(i_k) \right),$$

for $i_k \in \{1, 2, \dots, d\}$, assuming that the limit exists, and refer to r as the rank of x . Graphically, we represent it as

$$\mathbf{x} = \overbrace{\left(\cdots - \boxed{X} - \boxed{X} - \boxed{X} - \cdots \right)}_{\begin{array}{c} | \quad | \quad | \\ i_{-1} \quad i_0 \quad i_1 \end{array}}.$$

Note that even though \mathbf{x} contains an infinite number of cores, each core is completely defined by the d slices of X so that \mathbf{x} can be represented by a finite amount of data. A translational invariant iTR is also known as a uniform matrix product state [24]. In the remainder of the paper, we will only work with translational invariant iTRs and just call them iTRs for brevity.

3.3. Transfer matrix. The core tensor X of an iTR defines a special matrix called the *transfer matrix*, which plays a key role in many operations performed on the iTR, including Rayleigh quotient and residual calculations.

DEFINITION 3.4 (Transfer matrix). *Let \mathbf{x} be an iTR as in Definition 3.3. Then we define the transfer matrix T_X associated with \mathbf{x} as the $r^2 \times r^2$ matrix*

$$(3.1) \quad T_X := \sum_{i=1}^d X(i) \otimes X(i) = \begin{array}{c} \boxed{X} \\ | \\ \boxed{X} \end{array},$$

where $X(i)$ is the i th slice of X .

Multiplying T_X with a vector $v \in \mathbb{R}^{r^2}$ is equivalent to performing the summation $W = \sum_{i=1}^d X(i) V X(i)^T$, where V is obtained from reshaping v into an $r \times r$ matrix. It is known that the transfer matrix (3.1) defines a complete positive map [5, 20], which is a linear transformation that maps a positive semi-definite matrix V to another positive semi-definite matrix $X V X^T$. Under an additional irreducibility assumption, the dominant eigenvalue of T_X is simple (and positive); if we reshape the corresponding left or right eigenvector into a matrix, that matrix is symmetric positive definite [7, 8, 17]. In the following we will tacitly assume that the dominant eigenvalue is simple, which allows us to easily obtain the infinite power of T_X from its left and right eigenvectors.

LEMMA 3.5. *Let $\eta > 0$ be the simple dominant eigenvalue of T_X , with v_L and v_R being the corresponding left and right eigenvectors, respectively, normalized to satisfy $v_L^\top v_R = 1$. Then*

$$(3.2) \quad \lim_{k \rightarrow \infty} \left(\frac{T_X}{\eta} \right)^k = v_R v_L^\top.$$

Proof. By the assumptions, there are nonsingular matrices of the form $W_L = \begin{bmatrix} v_L & \bullet \end{bmatrix}$, $W_R = \begin{bmatrix} v_R & \bullet \end{bmatrix}$ such that

$$(3.3) \quad W_L^* T_X = \Lambda W_L^*, \quad T_X W_R = W_R \Lambda, \quad \Lambda = \begin{bmatrix} \eta & 0 \\ 0 & \Lambda_2 \end{bmatrix}, \quad W_L^* W_R = I,$$

where the spectral radius of Λ_2 is smaller than 1. Using that $W_R^{-1} = W_L^*$, this yields

$$\lim_{k \rightarrow \infty} \left(\frac{T_X}{\eta} \right)^k = \lim_{k \rightarrow \infty} \frac{1}{\eta^k} W_R \Lambda^k W_R^{-1} = \lim_{k \rightarrow \infty} \frac{1}{\eta^k} W_R \Lambda^k W_L^* = v_R v_L^\top,$$

which completes the proof. \square

COROLLARY 3.6 (Normalized iTR). *Let \mathbf{x} be an iTR as in Definition 3.3. Then \mathbf{x} is normalized, i.e., $\mathbf{x}^\top \mathbf{x} = 1$, if its corresponding transfer matrix T_X has a simple dominant eigenvalue $\eta = 1$.*

Proof. The proof directly follows from [Lemma 3.5](#), i.e.,

$$\mathbf{x}^\top \mathbf{x} = \left(\begin{array}{c} \cdots \text{---} \boxed{X} \text{---} \boxed{X} \text{---} \boxed{X} \text{---} \cdots \\ \cdots \text{---} \boxed{X} \text{---} \boxed{X} \text{---} \boxed{X} \text{---} \cdots \end{array} \right) = \text{Tr} \left[\lim_{k \rightarrow \infty} (T_X)^k \right] = \text{Tr} [v_R v_L^\top] = v_L^\top v_R = 1,$$

where we also used the trace property $\text{Tr}(AB) = \text{Tr}(BA)$. \square

When the dominant eigenvalue of the transfer matrix η is simple, $v_L^\top v_R \neq 0$ holds. We will assume that the eigenvectors v_L and v_R satisfy the normalization condition $v_L^\top v_R = 1$. A graphical depiction of the dominant left and right eigenvalue relation, and the normalization condition for $v_L =: \text{vec}(V_L)$, $v_R =: \text{vec}(V_R)$ are shown in [Figure 1](#).

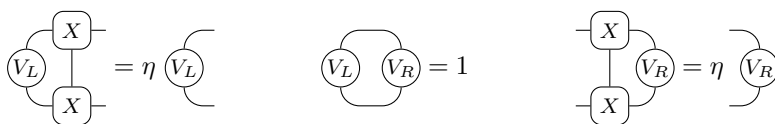


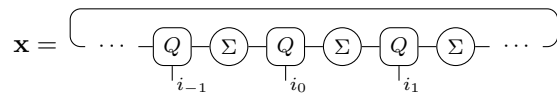
FIG. 1. Dominant eigenvalue relations of the transfer matrix and the normalization condition $v_L^\top v_R = 1$.

3.4. Canonical decomposition. Because we can insert the product of any nonsingular matrix S and its inverse between two consecutive cores of an iTR and redefine each slice as $S^{-1}X(i)S$, $i = 1, \dots, d$, the representation of an iTR is not unique. It is useful to define a canonical form that makes it easier to describe computations performed on iTRs¹.

DEFINITION 3.7 (Canonical form). Let \mathbf{x} be an iTR as in [Definition 3.3](#). We say that \mathbf{x} is in canonical form if it can be represented as

$$(3.4) \quad \mathbf{x}(\dots, i_{-1}, i_0, i_1, \dots) := \text{Tr} \left[\prod_{k=-\infty}^{+\infty} Q(i_k) \Sigma \right],$$

and graphically



where $Q(i) \in \mathbb{R}^{r \times r}$, for $i = 1, \dots, d$, and $\Sigma \in \mathbb{R}^{r \times r}$ is a diagonal matrix with decreasing non-negative real numbers on its diagonal and $\|\Sigma\|_F = 1$, such that the following left and right orthogonality conditions hold

$$(3.5) \quad \sum_{i=1}^d Q_L(i)^\top Q_L(i) = \eta I, \quad \sum_{i=1}^d Q_R(i) Q_R(i)^\top = \eta I,$$

with $Q_L(i) := \Sigma Q(i)$, $Q_R(i) := Q(i) \Sigma$, and $\eta \in \mathbb{R}$ being the dominant eigenvalue of the transfer matrix T_X .

¹We use a slightly different definition of the canonical form compared to [\[24\]](#) in order to ensure that a canonical iTR is always normalized to 1. The (mixed) canonical form introduced in [\[24\]](#) normalizes to $\|\Sigma^2\|_F^2$.

We call the 3rd-order tensor Q the orthogonal core of \mathbf{x} and Σ the corresponding singular value matrix, since it can be obtained from a singular value decomposition. The 3rd-order tensors Q_L and Q_R , defined in [Definition 3.7](#), are called the left and right orthogonal cores, respectively.

Before explaining how to compute the canonical form, we will list some properties. First, note that, by definition, Q and Σ satisfy the relations

$$(3.6) \quad \Sigma Q(i) \Sigma = Q_L(i) \Sigma = \Sigma Q_R(i),$$

for $i = 1, \dots, d$. The left and right canonical transfer matrices are defined as follows.

DEFINITION 3.8 (Canonical transfer matrices). *Let \mathbf{x} be an iTR in canonical form as in [Definition 3.7](#). Then we define its left and right canonical transfer matrices T_{Q_L} and T_{Q_R} as the following $r^2 \times r^2$ matrices*

$$(3.7) \quad T_{Q_L} := \sum_{i=1}^d Q_L(i) \otimes Q_L(i) = \begin{array}{c} \text{---} \textcircled{\Sigma} \text{---} \textcircled{Q} \text{---} \\ \text{---} \textcircled{\Sigma} \text{---} \textcircled{Q} \text{---} \end{array},$$

$$(3.8) \quad T_{Q_R} := \sum_{i=1}^d Q_R(i) \otimes Q_R(i) = \begin{array}{c} \text{---} \textcircled{Q} \text{---} \textcircled{\Sigma} \text{---} \\ \text{---} \textcircled{Q} \text{---} \textcircled{\Sigma} \text{---} \end{array},$$

with Q_L and Q_R defined as in [Definition 3.7](#).

The canonical transfer matrices, associated with an iTR in canonical form, as well as their dominant left and right eigenvectors, have the following fixed form.

LEMMA 3.9. *Let \mathbf{x} be an iTR in canonical form as in [Definition 3.7](#) with its corresponding canonical transfer matrices as in [Definition 3.8](#). Then,*

$$(3.9) \quad \text{vec}(I)^\top T_{Q_L} = \eta \text{vec}(I)^\top, \quad T_{Q_R} \text{vec}(I) = \eta \text{vec}(I),$$

$$(3.10) \quad T_{Q_L} \text{vec}(\Sigma^2) = \eta \text{vec}(\Sigma^2), \quad \text{vec}(\Sigma^2)^\top T_{Q_R} = \eta \text{vec}(\Sigma^2)^\top,$$

with $\text{vec}(I)$ being the dominant left eigenvector of T_{Q_L} and the dominant right eigenvector of T_{Q_R} , and $\text{vec}(\Sigma^2)$ being the dominant right eigenvector of T_{Q_L} and the dominant left eigenvector of T_{Q_R} .

Proof. The proof for the dominant right eigenvector of T_{Q_R} directly follows from vectorizing the second equality of [\(3.5\)](#):

$$\eta \text{vec}(I) = \text{vec} \left(\sum_{i=1}^d Q_R(i) Q_R(i)^\top \right) = \left(\sum_{i=1}^d Q_R(i) \otimes Q_R(i) \right) \text{vec}(I) = T_{Q_R} \text{vec}(I),$$

where we used [\(3.8\)](#) as well as relations between Kronecker products and vectorization:

$$(3.11) \quad \text{vec}(ABC) = (C^\top \otimes A) \text{vec}(B).$$

For the proof of the dominant left eigenvector of T_{Q_L} , we start from vectorizing the first equality of [\(3.5\)](#) and again apply [\(3.11\)](#) to obtain

$$(3.12) \quad \eta \text{vec}(I) = \text{vec} \left(\sum_{i=1}^d Q_L(i)^\top Q_L(i) \right) = \left(\sum_{i=1}^d Q_L(i)^\top \otimes Q_L(i)^\top \right) \text{vec}(I).$$

Transposing (3.12) and using (3.7) completes the proof of (3.9).

In order to prove that $\text{vec}(\Sigma^2)$ is the dominant right eigenvector of T_{Q_L} , we start again from the vectorization of the right equality of (3.5),

$$(3.13) \quad \text{vec} \left(\sum_{i=1}^d Q(i) \Sigma^2 Q(i)^\top \right) = \left(\sum_{i=1}^d Q(i) \otimes Q(i) \right) \text{vec}(\Sigma^2) = \eta \text{vec}(I),$$

where we substituted $Q_R(i) = Q(i)\Sigma$ and applied (3.11). Next, we multiply both sides of (3.13) from the left by $\Sigma \otimes \Sigma$, yielding

$$\underbrace{(\Sigma \otimes \Sigma) \left(\sum_{i=1}^d Q(i) \otimes Q(i) \right)}_{= T_{Q_L}} \text{vec}(\Sigma^2) = \eta (\Sigma \otimes \Sigma) \text{vec}(I) = \eta \text{vec}(\Sigma^2).$$

Finally, in order to prove that $\text{vec}(\Sigma^2)$ is also the dominant left eigenvector of T_{Q_R} , we start from the vectorization of the left equality of (3.5),

$$(3.14) \quad \text{vec} \left(\sum_{i=1}^d Q(i)^\top \Sigma^2 Q(i) \right) = \left(\sum_{i=1}^d Q(i)^\top \otimes Q(i)^\top \right) \text{vec}(\Sigma^2) = \eta \text{vec}(I),$$

where we substituted $Q_L(i) = \Sigma Q(i)$ and made use of the identity (3.11). Next, we multiply both sides of (3.14) from the left by $\Sigma \otimes \Sigma$ followed by a transposition, yielding

$$\text{vec}(\Sigma^2)^\top \underbrace{\left(\sum_{i=1}^d Q(i) \otimes Q(i) \right)}_{= T_{Q_R}} (\Sigma \otimes \Sigma) = \eta [(\Sigma \otimes \Sigma) \text{vec}(I)]^\top = \eta \text{vec}(\Sigma^2)^\top,$$

which proves (3.10) and completes the proof. \square

The eigenvalue decompositions of Lemma 3.9 are graphically shown in Figure 2. Note also that the left and right orthogonality conditions (3.5), defined by the canonical form, can be expressed in terms of the canonical transfer matrices and are equivalent to (3.9). Using the orthogonality conditions (3.5), we notice that computing the

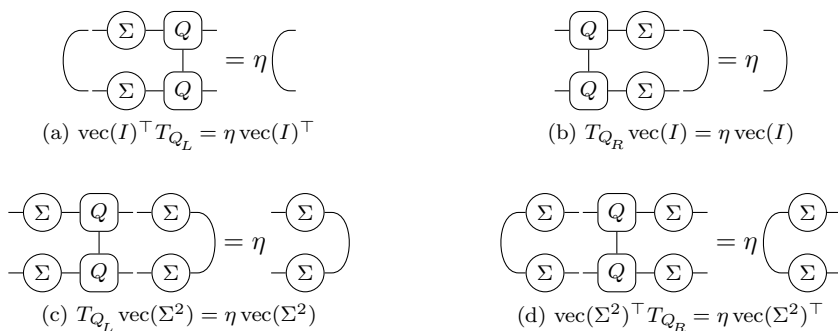


FIG. 2. Eigenvalue decompositions of the canonical transfer matrices.

canonical form of an iTR corresponds to finding matrices $Q(i)$ and a diagonal Σ so that

$$(3.15) \quad \sum_{i=1}^d Q(i)^\top \Sigma^2 Q(i) = \eta I = \sum_{i=1}^d Q(i) \Sigma^2 Q(i)^\top.$$

Algorithm 1 shows how the canonical decomposition of an iTR can be computed [14]. The complexity of **Algorithm 1** is dominated by step 1, which requires the computation of the dominant left and right eigenvectors of the $r^2 \times r^2$ transfer matrix T_X . In step 2, we use that the matricization of the dominant left and right eigenvectors, V_L and V_R , are positive definite matrices [8]. Using the properties $L^{-1} = R\tilde{\Sigma}$, $R^{-1} = \tilde{\Sigma}L$, $V_R = R\tilde{\Sigma}^2 R^\top$, and $V_L = L^\top \tilde{\Sigma}^2 L$, in combination with the identity (3.11), we can show that Q and Σ obtained in step 6 of **Algorithm 1** satisfy (3.15). Finally, we normalize the canonical iTR in step 7.

Algorithm 1: Canonical decomposition of iTR

Input : 3rd-order tensor X

Output: 3rd-order tensor Q and diagonal matrix Σ

1 Dominant left and right eigenvectors of transfer matrix T_X :

$$\text{vec}(V_L)^\top T_X = \eta \text{vec}(V_L)^\top, \quad T_X \text{vec}(V_R) = \eta \text{vec}(V_R).$$

2 Eigendecompositions of V_L and V_R : $V_L = U_L \Lambda_L U_L^\top, \quad V_R = U_R \Lambda_R U_R^\top.$

3 Form: $\tilde{U}_L = U_L \Lambda_L^{1/2}, \quad \tilde{U}_R = U_R \Lambda_R^{1/2}.$

4 Singular value decomposition: $V \tilde{\Sigma} W^\top = \tilde{U}_L^\top \tilde{U}_R.$

5 Form: $L = W^\top \tilde{U}_R^{-1}, \quad R = \tilde{U}_L^{-\top} V.$

6 Canonical form: $Q(i) = \|\tilde{\Sigma}\|_F L X(i) R, \quad \Sigma = \tilde{\Sigma} / \|\tilde{\Sigma}\|_F.$

7 Normalization: $Q(i) = Q(i) / \sqrt{\eta}.$

3.5. Frame matrix. Starting from an iTR in canonical form as in **Definition 3.7**, we can rewrite it as a product of an infinite-dimensional matrix with orthogonal columns, called the *frame matrix* [6, 12], and a finite vector of length equal to the number of elements in 1 core.

DEFINITION 3.10 (Frame matrix). *Let \mathbf{x} be a normalized iTR in canonical form as in **Definition 3.7**. Then we define its k th frame matrix as follows*

$$(3.16) \quad \mathbf{F}_{\neq k} := \left[\dots \underset{i_{k-2}}{\text{Q}} \text{---} \underset{i_{k-1}}{\Sigma} \text{---} \underset{i_{k-1}}{\text{Q}} \overset{j_{k-1}}{\text{---}} \overset{j_k}{\text{---}} \underset{i_k}{\text{---}} \overset{j_{k+1}}{\text{---}} \underset{i_{k+1}}{\text{Q}} \text{---} \underset{i_{k+1}}{\Sigma} \text{---} \dots \right].$$

Note that by this definition the frame matrix $\mathbf{F}_{\neq k}$ has an infinite number of rows, which are represented as downwards pointing legs, and dr^2 columns, which are represented as upwards pointing legs. Now the iTR \mathbf{x} can also be written as

$$(3.17) \quad \mathbf{x} = \mathbf{F}_{\neq k} \text{vec}(Q_c), \quad \text{---} \underset{i_c}{\text{Q}_c} \text{---} = \text{---} \underset{i_c}{\Sigma} \text{---} \underset{i_c}{\text{Q}} \text{---} \underset{i_c}{\Sigma} \text{---},$$

the $r^2 \times r^2$ matrices

$$(3.19) \quad T_{XY} := \sum_{i=1}^d \sum_{j=1}^d [X(i) \otimes X(i)] [Y(j) \otimes Y(j)] = \begin{array}{c} \text{---} \text{X} \text{---} \text{Y} \text{---} \\ | \quad | \\ \text{---} \text{X} \text{---} \text{Y} \text{---} \end{array},$$

$$(3.20) \quad T_{YX} := \sum_{i=1}^d \sum_{j=1}^d [Y(i) \otimes Y(i)] [X(j) \otimes X(j)] = \begin{array}{c} \text{---} \text{Y} \text{---} \text{X} \text{---} \\ | \quad | \\ \text{---} \text{Y} \text{---} \text{X} \text{---} \end{array},$$

where $X(i)$ is the i th slice of X and $Y(j)$ the j th slice of Y .

Note that the transfer matrices T_{XY} and T_{YX} of an iTR2 can also be expressed in terms of the 1-core transfer matrices, i.e., $T_{XY} = T_X T_Y$ and $T_{YX} = T_Y T_X$, where T_X is the transfer matrix formed by only using the core X and T_Y the transfer matrix formed by only using the core Y .

LEMMA 3.13. *Let \mathbf{x} be an iTR2 as in Definition 3.11 and assume that T_X and T_Y are nonsingular. Then its corresponding transfer matrices T_{XY} and T_{YX} , defined in Definition 3.12, have the same eigenvalues.*

Proof. We will show that every eigenvalue of T_{XY} is also an eigenvalue T_{YX} , and vice versa. First, assume that (λ, v) is an eigenpair of T_{XY} , $T_{XY}v = \lambda v$. Multiplying both sides from the left by T_Y , yields $T_Y T_X (T_Y v) = \lambda (T_Y v)$, hence, the pair $(\lambda, w := T_Y v)$ is an eigenpair of T_{YX} .

Similarly, assume that (λ, w) is an eigenpair of T_{YX} , $T_{YX}w = \lambda w$. Multiplying both sides from the left by T_X , yields again $T_X T_Y (T_X w) = \lambda (T_X w)$, hence, the pair $(\lambda, v := T_X w)$ is an eigenpair of T_{XY} . \square

We now define the canonical form of an iTR2. Since the canonical form is mainly used for normalized iTRs and iTR2s, we will assume that the dominant eigenvalue of its transfer matrices $\eta = 1$.

DEFINITION 3.14 (iTR2 canonical form). *Let \mathbf{x} be an iTR2 as in Definition 3.11, then \mathbf{x} is in canonical form if it can be represented as*

$$(3.21) \quad \mathbf{x}(\dots, i_0, i_1, i_2, i_3, \dots) := \text{Tr} \left[\prod_{k=-\infty}^{+\infty} Q(i_{2k}) \Sigma U(i_{2k+1}) \Omega \right],$$

and graphically

$$\mathbf{x} = \left(\dots \text{---} \underset{i_0}{\text{Q}} \text{---} \Sigma \text{---} \underset{i_1}{\text{U}} \text{---} \Omega \text{---} \underset{i_2}{\text{Q}} \text{---} \Sigma \text{---} \underset{i_3}{\text{U}} \text{---} \Omega \text{---} \dots \right)$$

where $Q(i), U(i) \in \mathbb{R}^{r \times r}$, for $i = 1, \dots, d$, and $\Sigma, \Omega \in \mathbb{R}^{r \times r}$ are diagonal matrices with decreasing non-negative real numbers on its diagonal and $\|\Sigma\|_F = \|\Omega\|_F = 1$, such that the following left and right orthogonality conditions hold

$$(3.22) \quad \sum_{i=1}^d Q_L(i)^\top Q_L(i) = I, \quad \sum_{i=1}^d Q_R(i) Q_R(i)^\top = I,$$

$$(3.23) \quad \sum_{i=1}^d U_L(i)^\top U_L(i) = I, \quad \sum_{i=1}^d U_R(i) U_R(i)^\top = I,$$

with $Q_L(i) := \Omega Q(i)$, $Q_R(i) := Q(i) \Sigma$, $U_L(i) := \Sigma U(i)$, and $U_R(i) := U(i) \Omega$.

Proof. We first rewrite (4.2) in matrix notation

$$(4.4) \quad \mathbf{x}^\top \mathbf{H}_k \mathbf{x} = \text{Tr} \left[\left(\prod_{\ell=-\infty}^{k-1} T_X \right) \tilde{M} \left(\prod_{\ell=k+2}^{+\infty} T_X \right) \right], \quad \tilde{M} := \begin{array}{c} \text{---} \text{X} \text{---} \text{X} \text{---} \\ | \quad | \\ \text{---} \text{M} \text{---} \\ | \quad | \\ \text{---} \text{X} \text{---} \text{X} \text{---} \end{array}.$$

It follows from Lemma 3.5 that

$$\mathbf{x}^\top \mathbf{H}_k \mathbf{x} = \text{Tr} \left[v_R v_L^\top \tilde{M} v_R v_L^\top \right] = \text{Tr} \left[v_L^\top \tilde{M} v_R v_L^\top v_R \right] = v_L^\top \tilde{M} v_R = \theta,$$

where we consecutively used the trace cyclic property $\text{Tr}(XYZ) = \text{Tr}(YZX)$ and the normalization of the left and right eigenvectors $v_L^\top v_R = 1$. \square

If \mathbf{x} is a normalized iTR, the evaluation of the Rayleigh quotient only requires multiplying the matrix \tilde{M} (4.4) from the left and right, respectively, with the left and right dominant eigenvectors of its corresponding transfer matrix T_X . In case \mathbf{x} is given in canonical form, the Rayleigh quotient simplifies further because there is no need to compute the left and right dominant eigenvectors of the transfer matrix, see Lemma 3.9.

COROLLARY 4.2 (Canonical iTR Rayleigh quotient). *Let \mathbf{x} be a normalized iTR in canonical form as in Definition 3.7 and its corresponding canonical transfer matrices as in Definition 3.8. Then the iTR Rayleigh quotient associated with the infinite-dimensional matrix \mathbf{H} (1.3) can be computed as follows*

$$(4.5) \quad \theta = \begin{array}{c} \text{---} \Sigma \text{---} Q \text{---} \Sigma \text{---} Q \text{---} \Sigma \text{---} \\ | \quad | \quad | \quad | \\ \text{---} \text{M} \text{---} \\ | \quad | \quad | \quad | \\ \text{---} \Sigma \text{---} Q \text{---} \Sigma \text{---} Q \text{---} \Sigma \text{---} \end{array},$$

where Q and Σ are given in Definition 3.7.

Proof. Since \mathbf{x} is in canonical form, the iTR Rayleigh quotient (4.2) takes the form

$$(4.6) \quad \mathbf{x}^\top \mathbf{H}_k \mathbf{x} = \begin{array}{c} \text{---} \left[\dots \text{---} Q \text{---} \Sigma \text{---} Q \text{---} \Sigma \text{---} Q \text{---} \Sigma \text{---} Q \text{---} \Sigma \text{---} \dots \right] \text{---} \\ | \quad | \quad | \quad | \\ \text{---} \text{M} \text{---} \\ | \quad | \quad | \quad | \\ \text{---} \left[\dots \text{---} Q \text{---} \Sigma \text{---} Q \text{---} \Sigma \text{---} Q \text{---} \Sigma \text{---} Q \text{---} \Sigma \text{---} \dots \right] \text{---} \end{array},$$

for arbitrary k . In matrix notation, this reads as

$$\mathbf{x}^\top \mathbf{H}_k \mathbf{x} = \text{Tr} \left[\left(\prod_{\ell=-\infty}^{k-1} T_{Q_R} \right) \tilde{M}_Q \left(\prod_{\ell=k+2}^{+\infty} T_{Q_R} \right) \right], \quad \tilde{M}_Q := \begin{array}{c} \text{---} Q \text{---} \Sigma \text{---} Q \text{---} \Sigma \text{---} \\ | \quad | \\ \text{---} \text{M} \text{---} \\ | \quad | \\ \text{---} Q \text{---} \Sigma \text{---} Q \text{---} \Sigma \text{---} \end{array}.$$

Using Lemma 3.5 together with the fact that $\text{vec}(\Sigma^2)$ and $\text{vec}(I)$ are the left and right dominant eigenvectors of T_{Q_R} , respectively, we obtain

$$\mathbf{x}^\top \mathbf{H}_k \mathbf{x} = \text{Tr} \left[\text{vec}(I) \text{vec}(\Sigma^2)^\top \tilde{M}_Q \text{vec}(I) \text{vec}(\Sigma^2)^\top \right] = \text{vec}(\Sigma^2)^\top \tilde{M}_Q \text{vec}(I) = \theta,$$

We start by projecting \mathbf{H} into the subspace spanned by the columns of the frame matrix, defined in [Definition 3.10](#). Due to the translational invariance of \mathbf{x} , we can choose an arbitrary k for the frame matrix. Therefore, without loss of generality, we set $k = 0$ for the remainder of this section. We define the projection of \mathbf{H} onto $\mathbf{F}_{\neq 0}$ as follows

$$(4.12) \quad H_{\neq 0} := \mathbf{F}_{\neq 0}^\top \mathbf{H} \mathbf{F}_{\neq 0} = \sum_{k=-\infty}^{+\infty} \mathbf{F}_{\neq 0}^\top \mathbf{H}_k \mathbf{F}_{\neq 0} =: \sum_{k=-\infty}^{+\infty} H_k.$$

where \mathbf{H}_k is defined in [\(1.3\)](#) and the matrices $H_k \in \mathbb{R}^{dr^2 \times dr^2}$ are obtained by projecting the corresponding \mathbf{H}_k onto $\mathbf{F}_{\neq 0}$. Depending on the relative position of the matrix M in each \mathbf{H}_k , with respect to index i_0 in $\mathbf{F}_{\neq 0}$, the matrices H_k have different expressions for each k , i.e.,

$$(4.13) \quad \begin{aligned} H_{-2-\ell} &= \text{Diagram 1}, & \ell = 0, 1, \dots, \\ H_{-1} &= \text{Diagram 2}, \\ H_0 &= \text{Diagram 3}, \\ H_{1+\ell} &= \text{Diagram 4}, & \ell = 0, 1, \dots, \end{aligned}$$

with

$$(4.14) \quad \text{Diagram 5} := \text{Diagram 6}, \quad \text{Diagram 7} := \text{Diagram 8}.$$

Note that, because the transfer matrices T_{Q_L} and T_{Q_R} have the dominant eigenvalue 1, the infinite sums

$$(4.15) \quad \sum_{\ell=0}^{+\infty} (T_{Q_L})^\ell, \quad \text{and} \quad \sum_{\ell=0}^{+\infty} (T_{Q_R})^\ell$$

diverge, hence, the infinite sum in [\(4.12\)](#) also diverges.

On the other hand, we can show that for every H_k in [\(4.13\)](#),

$$\text{vec}(Q_c)^\top H_k \text{vec}(Q_c) = \theta,$$

where θ is the the Rayleigh quotient (4.5) and Q_c the canonical center core (3.17). Therefore, we define the iTR residual as follows

$$(4.16) \quad \text{Res} := \sum_{k=-\infty}^{+\infty} \left(H_k \text{vec}(Q_c) - \theta \text{vec}(Q_c) \right) =: \sum_{k=-\infty}^{+\infty} \text{Res}_k.$$

The following theorem shows how to construct this residual and proves that, in contrast to the infinite sum in (4.12), the iTR residual defined in (4.16) does converge.

THEOREM 4.4 (Residual). *Let \mathbf{x} be a normalized nonzero canonical iTR as in Definition 3.7. Then the residual for a given infinite-dimensional matrix \mathbf{H} (1.3) is given by*

$$(4.17) \quad \text{Res} = \begin{array}{c} \text{Diagram 1} \\ + \\ \text{Diagram 2} \\ + \\ \text{Diagram 3} \\ + \\ \text{Diagram 4} \\ - 4\theta \text{Diagram 5} \end{array},$$

where θ is the Rayleigh quotient (4.5), Q_c the canonical center core (3.17), and

$$(4.18) \quad \text{vec}(L)^\top := \text{vec}(l)^\top \left[I - \tilde{T}_{Q_L} \right]^{-1}, \quad \tilde{T}_{Q_L} := T_{Q_L} - \text{vec}(\Sigma^2) \text{vec}(I)^\top,$$

$$(4.19) \quad \text{vec}(R) := \left[I - \tilde{T}_{Q_R} \right]^{-1} \text{vec}(r), \quad \tilde{T}_{Q_R} := T_{Q_R} - \text{vec}(I) \text{vec}(\Sigma^2)^\top.$$

with l and r are defined by the diagrams given in (4.13).

Proof. Since each term in the infinite sum of (4.16) is defined as the difference $\text{Res}_k = H_k \text{vec}(Q_c) - \theta \text{vec}(Q_c)$, we immediately obtain from (4.13) that the 2nd and 3rd term in (4.17) are equal to $H_{-1} \text{vec}(Q_c)$ and $H_0 \text{vec}(Q_c)$, respectively. Next, we will prove that $\sum_{k=-\infty}^{-2} \text{Res}_k$ yields the 1st term in (4.17) minus $\theta \text{vec}(Q_c)$, and $\sum_{k=1}^{+\infty} \text{Res}_k$ yields the 4th term minus $\theta \text{vec}(Q_c)$. We show that both infinite sums converge.

By using (4.5) and (4.13), we diagrammatically rewrite $\theta \text{vec}(Q_c)$ in the following factored form

$$\theta \text{vec}(Q_c) = \begin{array}{c} \text{Diagram 1} \\ \text{Diagram 2} \end{array} = \begin{array}{c} \text{Diagram 3} \\ \underbrace{\text{Diagram 4}}_{\text{vec}(\Sigma^2) \text{vec}(I)^\top} \end{array},$$

yielding

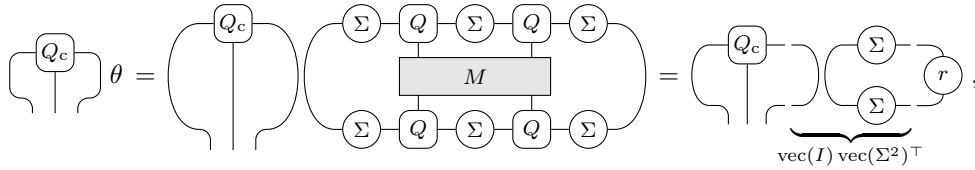
$$(4.20) \quad \text{Res}_{-2-\ell} = \begin{array}{c} \text{Diagram 1} \\ \text{Diagram 2} \end{array} - \theta \text{vec}(Q_c) = \begin{array}{c} \text{Diagram 3} \\ \text{Diagram 4} \end{array},$$

where $(\tilde{T}_{Q_L})^\ell = (T_{Q_L})^\ell - \text{vec}(\Sigma^2) \text{vec}(I)^\top$ for $\ell = 1, 2, \dots$. Because $\text{vec}(I)$ and $\text{vec}(\Sigma^2)$ are the left and right eigenvectors associated with the dominant eigenvalue 1 of T_{Q_L} , as shown in Lemma 3.9, the largest eigenvalue of the deflated matrix \tilde{T}_{Q_L} is less than 1 (in magnitude). Hence, in contrast to (4.15), the geometric series of \tilde{T}_{Q_L} converges, yielding

$$\sum_{\ell=0}^{+\infty} (\tilde{T}_{Q_L})^\ell = [I - \tilde{T}_{Q_L}]^{-1}.$$

Note that this sum starts from 0 and (4.20) starts from 1. Consequently, the infinite sum $\sum_{k=-\infty}^{-2} \text{Res}_k$ yields the 1st term in (4.17) minus $\theta \text{vec}(Q_c)$, where L is defined by (4.18).

For the remaining part of the proof, we rewrite $\text{vec}(Q_c)\theta$ as



yielding

$$(4.21) \quad \text{Res}_{1+\ell} = \left(\text{Diagram of } (T_{Q_R})^\ell \right) - \left(\text{Diagram of } \text{vec}(Q_c)\theta \right) = \left(\text{Diagram of } (\tilde{T}_{Q_R})^\ell \right),$$

for $\ell = 1, 2, \dots$. Using similar arguments as before, we can show that the geometric series of \tilde{T}_{Q_R} converges and that the infinite sum $\sum_{k=1}^{+\infty} \text{Res}_k$ yields the 4th term in (4.17) minus $\theta \text{vec}(Q_c)$. Remark that the term $\theta \text{vec}(Q_c)$ in Res_k always gets incorporated in \tilde{T}_{Q_L} or \tilde{T}_{Q_R} , except for $k = -2, -1, 0, 1$, yielding the 5th term in (4.17). This completes the proof. \square

In order to define the residual for a Ritz pair (θ, \mathbf{x}) with \mathbf{x} being an iTR2, we first introduce the frame matrices $\mathbf{F}_{\neq Q}$ and $\mathbf{F}_{\neq U}$ which allow us to rewrite \mathbf{x} as follows

$$(4.22) \quad \mathbf{x} = \mathbf{F}_{\neq Q} \text{vec}(Q_c) = \mathbf{F}_{\neq U} \text{vec}(U_c),$$

where $\mathbf{F}_{\neq Q}^\top \mathbf{F}_{\neq Q} = \mathbf{F}_{\neq U}^\top \mathbf{F}_{\neq U} = I$ and the canonical center cores Q_c and U_c are

$$(4.23) \quad \text{Diagram of } Q_c = \text{Diagram of } \Omega - Q - \Sigma, \quad \text{Diagram of } U_c = \text{Diagram of } \Sigma - U - \Omega.$$

respectively. Next, we define the residual in an average sense as follows

$$\begin{aligned} \text{Res} &= \frac{1}{2} \sum_{k=-\infty}^{+\infty} \left(\mathbf{F}_{\neq Q}^\top \mathbf{H}_k \mathbf{F}_{\neq Q} \text{vec}(Q_c) - \theta \text{vec}(Q_c) \right) + \\ &\quad \frac{1}{2} \sum_{k=-\infty}^{+\infty} \left(\mathbf{F}_{\neq U}^\top \mathbf{H}_k \mathbf{F}_{\neq U} \text{vec}(U_c) - \theta \text{vec}(U_c) \right), \end{aligned}$$

where θ is the Rayleigh quotient (4.11), and Q_c and U_c the canonical center cores (4.23). The following theorem summarizes how to compute this residual.

THEOREM 4.5 (iTR2 residual). *Let \mathbf{x} be a normalized nonzero canonical iTR2 as in Definition 3.14. Then the residual for a given infinite-dimensional matrix \mathbf{H} (1.3) is given by*

$$(4.24) \quad \begin{aligned} \text{Res} = & \frac{1}{2} \left(L_Q \right) + \frac{1}{2} \left(\begin{array}{c} \Sigma \quad U \quad \Omega \quad Q \quad \Sigma \\ \text{---} \text{---} \text{---} \text{---} \text{---} \\ \text{---} \text{---} \text{---} \text{---} \text{---} \\ \Sigma \quad U \end{array} \right) + \\ & \frac{1}{2} \left(\begin{array}{c} \Omega \quad Q \quad \Sigma \quad U \quad \Omega \\ \text{---} \text{---} \text{---} \text{---} \text{---} \\ \text{---} \text{---} \text{---} \text{---} \text{---} \\ U \quad \Omega \end{array} \right) + \frac{1}{2} \left(\begin{array}{c} Q_c \\ \text{---} \text{---} \text{---} \\ R_Q \end{array} \right) - 3\theta \left(\begin{array}{c} Q_c \\ \text{---} \text{---} \\ \end{array} \right) + \\ & \frac{1}{2} \left(L_U \right) + \frac{1}{2} \left(\begin{array}{c} \Omega \quad Q \quad \Sigma \quad U \quad \Omega \\ \text{---} \text{---} \text{---} \text{---} \text{---} \\ \text{---} \text{---} \text{---} \text{---} \text{---} \\ \Omega \quad Q \end{array} \right) + \\ & \frac{1}{2} \left(\begin{array}{c} \Sigma \quad U \quad \Omega \quad Q \quad \Sigma \\ \text{---} \text{---} \text{---} \text{---} \text{---} \\ \text{---} \text{---} \text{---} \text{---} \text{---} \\ Q \quad \Sigma \end{array} \right) + \frac{1}{2} \left(\begin{array}{c} U_c \\ \text{---} \text{---} \text{---} \\ R_U \end{array} \right) - 3\theta \left(\begin{array}{c} U_c \\ \text{---} \text{---} \\ \end{array} \right), \end{aligned}$$

where θ is the Rayleigh quotient (4.11), Q_c and U_c the canonical center cores (4.23),

$$(4.25) \quad \begin{aligned} \text{vec}(L_Q)^\top &:= \left[\text{vec}(l_Q)^\top + \text{vec}(l_U)^\top T_{U_L} \right] \left[I - \tilde{T}_{Q_L U_L} \right]^{-1}, \\ \text{vec}(L_U)^\top &:= \left[\text{vec}(l_U)^\top + \text{vec}(l_Q)^\top T_{Q_L} \right] \left[I - \tilde{T}_{U_L Q_L} \right]^{-1}, \\ \text{vec}(R_Q) &:= \left[I - \tilde{T}_{U_R Q_R} \right]^{-1} \left[\text{vec}(r_U) + T_{U_R} \text{vec}(r_Q) \right], \\ \text{vec}(R_U) &:= \left[I - \tilde{T}_{Q_R U_R} \right]^{-1} \left[\text{vec}(r_Q) + T_{Q_R} \text{vec}(r_U) \right], \end{aligned}$$

with

$$\begin{aligned} \tilde{T}_{Q_L U_L} &:= T_{Q_L U_L} - \text{vec}(\Omega^2) \text{vec}(I)^\top, & \tilde{T}_{Q_R U_R} &:= T_{Q_R U_R} - \text{vec}(I) \text{vec}(\Omega^2)^\top, \\ \tilde{T}_{U_L Q_L} &:= T_{U_L Q_L} - \text{vec}(\Sigma^2) \text{vec}(I)^\top, & \tilde{T}_{U_R Q_R} &:= T_{U_R Q_R} - \text{vec}(I) \text{vec}(\Sigma^2)^\top, \end{aligned}$$

and

$$\begin{aligned} l_Q &:= \left(\begin{array}{c} \Omega \quad Q \quad \Sigma \quad U \\ \text{---} \text{---} \text{---} \text{---} \\ \text{---} \text{---} \text{---} \text{---} \\ \Omega \quad Q \quad \Sigma \quad U \end{array} \right), & r_Q &:= \left(\begin{array}{c} \Sigma \quad U \quad \Omega \quad Q \\ \text{---} \text{---} \text{---} \text{---} \\ \text{---} \text{---} \text{---} \text{---} \\ \Sigma \quad U \quad \Omega \quad Q \end{array} \right), \\ l_U &:= \left(\begin{array}{c} \Sigma \quad U \quad \Omega \quad Q \\ \text{---} \text{---} \text{---} \text{---} \\ \text{---} \text{---} \text{---} \text{---} \\ \Sigma \quad U \quad \Omega \quad Q \end{array} \right), & r_U &:= \left(\begin{array}{c} \Omega \quad Q \quad \Sigma \quad U \\ \text{---} \text{---} \text{---} \text{---} \\ \text{---} \text{---} \text{---} \text{---} \\ \Omega \quad Q \quad \Sigma \quad U \end{array} \right). \end{aligned}$$

Proof. The proof is similar to the one for Theorem 4.4. \square

5. Power method. One way to compute the algebraically smallest eigenvalue λ_1 of a symmetric positive definite matrix \mathbf{H} is to apply the power method to the matrix exponential $e^{-\mathbf{H}}$. If λ_1 is simple, the power method converges linearly to the desired eigenpair (λ_1, \mathbf{x}) at the rate $e^{\lambda_2 - \lambda_1}$. This approach is generally not recommended because working with the matrix exponential $e^{-\mathbf{H}}$ can be costly. In fact, computing $e^{-\mathbf{H}}$ or applying $e^{-\mathbf{H}}$ to a vector may be harder than computing selected eigenvalues of \mathbf{H} . However, when \mathbf{H} has the structure exhibited in (1.3), $e^{-\mathbf{H}t}$ may be approximated by a simpler form that makes it possible to (approximately) perform a power iteration for $e^{-\mathbf{H}t}$ if t is sufficiently small.

Throughout this section, we will make use of iTR matrices, which are graphically represented as follows

$$\mathbf{A} = \cdots \begin{array}{c} | \\ \text{---} \boxed{A} \text{---} \\ | \\ j_{-1} \end{array} \begin{array}{c} | \\ \text{---} \boxed{A} \text{---} \\ | \\ j_0 \end{array} \begin{array}{c} | \\ \text{---} \boxed{A} \text{---} \\ | \\ j_1 \end{array} \cdots ,$$

where all indices i_k, j_k run from 1 to d and each $A(j, i)$ is a matrix of size $r \times r$, with r referred to as the *rank* of \mathbf{A} .

5.1. Approximating $\exp(-\mathbf{H}t)$ by matrix splitting. We now discuss how to approximate the operation $e^{-\mathbf{H}t}\mathbf{x}$, with \mathbf{x} being an iTR, which is required in a single step of the power iteration. Because the terms \mathbf{H}_k in the sum $\mathbf{H} = \sum_k \mathbf{H}_k$ do not commute, the expressions $e^{-\mathbf{H}t}$ and $\cdots e^{-\mathbf{H}_{k-1}t} e^{-\mathbf{H}_k t} e^{-\mathbf{H}_{k+1}t} \cdots$ are not the same but they can be expected to be close for small t . Indeed, the Lie product formula, also known as Suzuki–Trotter splitting, states that

$$e^{(A+B)t} = e^{At}e^{Bt} + \mathcal{O}(t^2),$$

holds for square matrices A and B . This suggest the following approximation:

$$(5.1) \quad e^{-\mathbf{H}t} \approx \prod_{k=-\infty}^{+\infty} e^{-\mathbf{H}_k t}, \quad t \approx 0.$$

In the physics literature, t is viewed as an imaginary time variable and, hence, $e^{-\mathbf{H}t}$ is often referred to as imaginary time evolution.

Let us first assume that the matrices \mathbf{H}_k only act on one site, that is,

$$\mathbf{H}_k = \cdots \otimes I_d \otimes I_d \otimes A_k \otimes I_d \otimes I_d \otimes \cdots, \quad A_k = A \in \mathbb{R}^{d \times d}.$$

By making use of the identity $e^{I \otimes A \otimes I} = I \otimes e^A \otimes I$, the matrix exponentials $e^{-\mathbf{H}_k t}$ can be simplified as follows

$$e^{-\mathbf{H}_k t} = \cdots \otimes I \otimes I \otimes e^{-At} \otimes I \otimes I \otimes \cdots.$$

In turn, the infinite product in (5.1) is the rank-1 iTR matrix

$$\prod_{k=-\infty}^{+\infty} e^{-\mathbf{H}_k t} = \cdots \otimes e^{-At} \otimes e^{-At} \otimes e^{-At} \otimes \cdots = \cdots \begin{array}{c} | \\ \text{---} \boxed{e^{-At}} \text{---} \\ | \\ j_{-1} \end{array} \begin{array}{c} | \\ \text{---} \boxed{e^{-At}} \text{---} \\ | \\ j_0 \end{array} \begin{array}{c} | \\ \text{---} \boxed{e^{-At}} \text{---} \\ | \\ j_1 \end{array} \cdots ,$$

where the dotted lines correspond to rank $r = 1$. Hence, if \mathbf{x} is an iTR, the product

$$(5.2) \quad \mathbf{y} = \left(\prod_{k=-\infty}^{+\infty} e^{-\mathbf{H}_k t} \right) \mathbf{x},$$

which can be computed in the same way as (5.2) by reformulating \mathbf{x} as an iTR2 with 2 cores X , i.e., combining the $(2k+1)$ st and $(2k+2)$ nd cores into a *supercore* \mathcal{X} of dimension $r \times d^2 \times r$. Hence, (5.9) only requires the left multiplication of the slices of the new supercore with the $d^2 \times d^2$ matrix e^{-Mt}

$$\begin{array}{c} \text{---} \mathcal{Y}_o \text{---} \\ \downarrow d^2 \\ \text{---} \mathcal{X} \text{---} \\ \downarrow \\ \boxed{e^{-Mt}} \\ \downarrow \end{array}, \quad \text{with} \quad \begin{array}{c} \text{---} \mathcal{X} \text{---} \\ \downarrow d^2 \\ \text{---} X \text{---} X \text{---} \\ \downarrow d \quad \downarrow d \end{array},$$

where d and d^2 next to the crossed out legs correspond to the size of the (super)cores. Thereafter, we only need to multiply the even terms. However, directly applying

$$(5.10) \quad \mathbf{y} = \left(\prod_{k=-\infty}^{+\infty} e^{-\mathbf{H}_{2k}t} \right) \mathbf{y}_o$$

is not possible because the supercores \mathcal{Y}_o are formed by combining the indices $(2k+1, 2k+2)$, while (5.7) requires the indices $(2k, 2k+1)$ to be combined. Therefore, we first need to split up the supercore of \mathbf{y}_o back into 2 normal cores, followed by a new and different recombination of the cores in order to carry out (5.10) efficiently.

Note that the size of \mathcal{Y}_o is $r \times d^2 \times r$ and in order to split it up into 2 cores of size $r \times d \times r$, we necessarily need to perform an approximation. A possible way to achieve this is by first reshaping \mathcal{Y}_o into an $rd \times rd$ matrix C , next approximating C by a rank- r factorization

$$C \approx C_1 C_2^\top,$$

where $C_1, C_2 \in \mathbb{R}^{dr \times r}$, and finally reshaping the factors C_1 and C_2 into 3rd-order tensors

$$\begin{array}{c} \text{---} \mathcal{Y}_o \text{---} \\ \downarrow d^2 \\ \text{---} C \text{---} \\ \downarrow rd \\ \text{---} C_1 \text{---} C_2^\top \text{---} \\ \downarrow r \quad \downarrow rd \\ \text{---} Y_{1o} \text{---} Y_{2o} \text{---} \\ \downarrow d \quad \downarrow d \end{array}.$$

In order words, \mathbf{y}_o is approximated by

$$\tilde{\mathbf{y}}_o = \left[\dots \text{---} Y_{1o} \text{---} Y_{2o} \text{---} Y_{1o} \text{---} Y_{2o} \text{---} \dots \right].$$

$\downarrow_{i_{2k-1}} \quad \downarrow_{i_{2k}} \quad \downarrow_{i_{2k+1}} \quad \downarrow_{i_{2k+2}}$

Consequently, we can now approximate (5.10) by replacing \mathbf{y}_o with $\tilde{\mathbf{y}}_o$

$$\begin{array}{c} \text{---} \mathcal{Y} \text{---} \\ \downarrow d^2 \\ \text{---} \tilde{\mathcal{Y}}_o \text{---} \\ \downarrow \\ \boxed{e^{-Mt}} \\ \downarrow \end{array}, \quad \text{with} \quad \begin{array}{c} \text{---} \tilde{\mathcal{Y}}_o \text{---} \\ \downarrow d^2 \\ \text{---} Y_{2o} \text{---} Y_{1o} \text{---} \\ \downarrow d \quad \downarrow d \end{array}.$$

In the final step, we split the supercore \mathcal{Y} into 2 cores Y_2 and Y_1

$$\begin{array}{c} \text{---} \mathcal{Y} \text{---} \\ \downarrow d^2 \\ \text{---} D \text{---} \\ \downarrow rd \\ \text{---} D_1 \text{---} D_2 \text{---} \\ \downarrow r \quad \downarrow rd \\ \text{---} Y_2 \text{---} Y_1 \text{---} \\ \downarrow d \quad \downarrow d \end{array}.$$

or in order words, \mathbf{y} is approximated by

$$\tilde{\mathbf{y}} = \left[\dots \text{---} Y_2 \text{---} Y_1 \text{---} Y_2 \text{---} Y_1 \text{---} \dots \right].$$

$\downarrow_{i_{2k}} \quad \downarrow_{i_{2k+1}} \quad \downarrow_{i_{2k+2}} \quad \downarrow_{i_{2k+3}}$

Remark that, although we started with an iTR \mathbf{x} , the result of applying $e^{-\mathbf{H}t}$ to it is an iTR2. Therefore, in [Figure 3](#) we graphically illustrate the application of [\(5.1\)](#) to an iTR2 with cores X_1 and X_2 . Due to the translational invariance, we only need to apply e^{-Mt} twice in order to compute $\tilde{\mathbf{y}}$, which is indicated in black. The computation indicated in gray can completely be ignored, so that the multiplication $\mathbf{y} = e^{-\mathbf{H}t}\mathbf{x}$ can be computed in an efficient way.

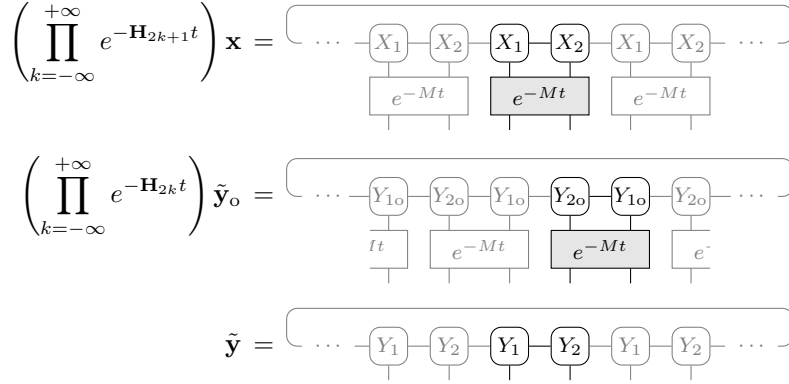


FIG. 3. The matrix–vector operation $\mathbf{y} = e^{-\mathbf{H}t}\mathbf{x}$.

5.2. Algorithm. As illustrated in [Figure 3](#), we only need to operate on 1 supercore at a time. Instead of working with supercores involving X_1, X_2 and Y_{2o}, Y_{1o} , respectively, we will operate on the following canonical center supercores \mathcal{X}_{1c} and \mathcal{X}_{2c} :

$$\mathcal{X}_{1c} = \left(\Omega - Q - U - \Sigma - \Omega \right), \quad \text{and} \quad \mathcal{X}_{2c} = \left(\Sigma - U - Q - \Omega - \Sigma \right),$$

respectively, so that their corresponding frame matrices are orthogonal.

We only describe the application of the odd part of $e^{-\mathbf{H}t}$ onto \mathcal{X}_c , since the even part can be performed in exactly the same way by interchanging Q, U and Σ, Ω , respectively. The computation consists of 5 steps as illustrated in [Figure 4](#). In step 1, the canonical center supercore \mathcal{X}_{1c} is formed. Next, we apply e^{-Mt} to it in step 2, followed by reshaping the resulting supercore \mathcal{Y}_{1c} into a matrix. In step 3, we approximate the matrix representation of \mathcal{Y}_{1c} by a truncated SVD, with the diagonal matrix S_r containing only the r largest singular values, followed by reshaping the left and right singular vectors W and V into 3rd-order tensors, i.e., cores. Then in step 4, in order to update the cores Q and U by W_Ω and V_Ω^\top , respectively, and the diagonal matrix Σ by S_r , we transform the result of step 3 into the form of step 1 by left and right multiplying W and V^\top , respectively, by Ω^{-1} . Note that, although the resulting form resembles the form of step 1, the former is not in canonical form yet. Therefore, we update in step 5 both cores Q_\star and U_\star , and both diagonal matrices Σ_\star and Ω_\star to bring the updated iTR2 again in canonical form.

We now have all components to state the method for computing the smallest eigenvalue of [\(1.3\)](#). Due to the approximation made by the Suzuki–Trotter splitting of $e^{-\mathbf{H}t}$ and the rank truncation for splitting a supercore into 2 normal cores, the multiplication $\mathbf{y} = e^{-\mathbf{H}t}\mathbf{x}$ is inexact. Even when t is fixed, the error introduced by the rank truncation is different in each iteration and results in the application of a slightly different operator every iteration. [Algorithm 3](#) shows the outline of

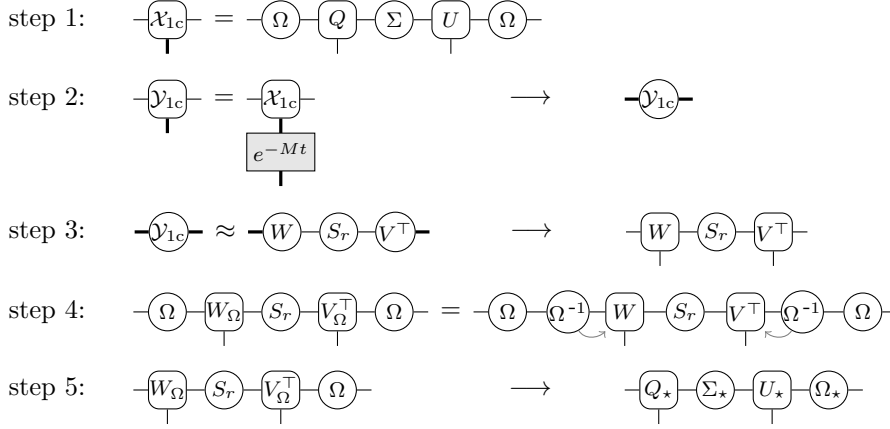


FIG. 4. The odd part of the matrix–vector operation $\mathbf{y} = e^{-\mathbf{H}t}\mathbf{x}$, where \mathbf{x} is given in canonical iTR2 form. Note that the even part corresponds to interchanging the cores Q and U , and the diagonal matrices Σ and Ω , respectively. (1) Forming the canonical center supercore. (2) Applying the matrix exponential followed by reshaping the result into a matrix. (3) Performing a truncated SVD and reshaping the singular vectors into cores. (4) Updating the cores and the central diagonal matrix, while keeping Ω unchanged. (5) Computing the canonical iTR2 form.

the power method for computing the smallest eigenvalue of (1.3). This algorithm takes a canonical iTR2 as starting vector and returns the Rayleigh quotient and its corresponding eigenvector in canonical iTR2 form. In every iteration of Algorithm 3, we apply the matrix exponential e^{-Mt} twice, according to Figure 4, followed by the computation of the Rayleigh quotient and residual.

Algorithm 3: iTR power method

Input : Canonical iTR2 with cores $Q, U \in \mathbb{R}^{r \times d \times r}$ and $\Sigma, \Omega \in \mathbb{R}^{r \times r}$

Nearest neighbor interaction matrix M and initial timestep t

Output: Rayleigh quotient and corresponding eigenvector in canonical iTR2

while not converged do

- 1 | Apply e^{-Mt} to supercore \mathcal{X}_{1c} according to Figure 4.
- 2 | Apply e^{-Mt} to supercore \mathcal{X}_{2c} according to Figure 4.
- 3 | Compute Rayleigh quotient θ as in (4.11).
- 4 | Check convergence based on residual (4.24).
- 5 | Update t .

end

As we will show in the numerical experiments, the time step t can have a significant effect on the convergence and accuracy of the Rayleigh quotient. On the one hand, when t is chosen very small then the eigenvalues of $e^{-\mathbf{H}t}$ are close to 1 and, in turn, the gap between the smallest and the second smallest eigenvalue becomes small, leading to a high number of iterations. On the other hand, if the time step is chosen too large, the convergence of Algorithm 3 stagnates prematurely due to the dominating Suzuki–Trotter splitting error. It is therefore recommended to adapt and decrease the time step t in the course of the algorithm. By starting with a relative large t , the

power method will stagnate in a small number of iterations. We can use the iTR2 residual for detecting stagnation. Next, we decrease t and continue the power method with the already obtained approximate eigenvector. By updating t and using more accurate approximate eigenvectors for smaller t , we will be able to reduce the total number of iterations.

5.3. Computational considerations. Most operations of [Algorithm 3](#) can be efficiently implemented involving only 3rd-order tensors of size $r \times d \times r$, such as steps 1–4 in [Figure 4](#) and the Rayleigh quotient. On the other hand, step 5 in [Figure 4](#) and the computation of the residual involve transfer matrices of size $r^2 \times r^2$. The former requires computing dominant eigenvectors of the left and right transfer matrices and the latter needs linear systems solves involving the same matrices. In practice, we can use the relation [\(3.11\)](#) to avoid forming these $r^2 \times r^2$ matrices explicitly and rewrite everything in terms of only $r \times r$ matrices. However, even for low values of $r \approx 10$, more than 90% of the wall clock time is still spent on these operations involving the transfer matrices. Therefore, we will make use of iterative methods for computing the dominant eigenvectors and the residual. We could choose not to compute the residual in every iteration but the cost for transforming the updated iTR2 to canonical form remains.

Therefore, we also propose a second variant of the power method that only works with standard iTR2s, i.e., ignoring step 5 in [Figure 4](#) such that the updated cores are $Q_\star := W_\Omega$ and $U_\star := V_\Omega^\top$, and the updated diagonal matrices are $\Sigma_\star := S_r$ and $\Omega_\star := \Omega$. Note that in this case only 1 of the 2 diagonal matrices is updated, hence the resulting iTR2 will, in general, not satisfy all the orthogonality conditions of [Definition 3.14](#). However, due to the alternating singular value decompositions on \mathcal{Y}_{1c} and \mathcal{Y}_{2c} , we observe that the resulting iTR2 converges to canonical form. As a result, we can still use the relatively cheap canonical Rayleigh quotient [\(4.11\)](#) compared to the standard Rayleigh quotient [\(4.10\)](#) which would again require the computation of dominant eigenvectors of the transfer matrices.

Note that in the iTEBD algorithm described in [\[21, 14\]](#) the matrix-vector operation $\mathbf{y} = e^{-\mathbf{H}t}\mathbf{x}$ is implemented in a slightly different way. Instead of bringing the updated iTR2 to canonical form, as done in step 5 in [Figure 4](#), the iTR2 is directly transformed to canonical form right after step 2 and before the truncation is applied in step 3. Hence, the resulting iTR2 is only approximately in canonical form.

6. Numerical experiments. In this section we illustrate the power method, outlined in [Algorithm 3](#), for 3 examples: the one-dimensional Ising model with a transverse field, the spin $S = 1$ Heisenberg isotropic antiferromagnetic model, and the spin $S = 1/2$ Heisenberg model.

All numerical experiments are performed in MATLAB version 9.6.0 (R2019a) on a MacBook Pro running an Intel(R) Core(TM) i7-5557U CPU @ 3.1 GHz dual core processor with 16 GB RAM. The dominant eigenvectors of the transfer matrices are computed via `eigs` and the linear systems for computing the residual in [\(4.25\)](#) are solved via `gmres` with tolerance $1e-8$.

6.1. One-dimensional transverse field Ising model. We start with the one-dimensional transverse field Ising model and corresponding infinite-dimensional Hamiltonian

$$(6.1) \quad \mathbf{H} = - \sum_{k=-\infty}^{+\infty} \cdots \otimes I \otimes \sigma_z \otimes \sigma_z \otimes I \otimes \cdots - g \sum_{k=-\infty}^{+\infty} \cdots \otimes I \otimes \sigma_x \otimes I \otimes \cdots$$

where $\sigma_x = \begin{bmatrix} 0 & 1 \\ 1 & 0 \end{bmatrix}$ and $\sigma_z = \begin{bmatrix} 1 & 0 \\ 0 & -1 \end{bmatrix}$ are the 1st and 3rd Pauli matrices, respectively, and the following 4×4 symmetric matrix

$$M = \begin{bmatrix} -1 & -g & 0 & 0 \\ -g & 1 & 0 & 0 \\ 0 & 0 & 1 & -g \\ 0 & 0 & -g & -1 \end{bmatrix}$$

as nearest neighbor interaction matrix in the notation of (1.3). We choose the parameter $g = 2$. The exact solution of the smallest eigenvalue of (6.1) is [18]

$$\lambda_0(g) = -\frac{1}{2\pi} \int_{-\pi}^{\pi} \sqrt{1 + g^2 - 2g \cos x} dx, \quad \lambda_0(2) \approx -2.127088819946730.$$

In the first experiment, we compare the 2 variants of Algorithm 3, i.e., the canonical variant where we always convert the result of applying e^{-Mt} back into canonical iTR2 form and the non-canonical variant where we skip step 5 in Figure 4. In order to improve the numerical stability in the latter one, we normalize the diagonal matrices to have unit Frobenius norm. Figure 5a shows the Rayleigh quotient θ and its difference with the exact solution as a function of the iteration count. Note that the results for both variants of Algorithm 3 are indistinguishable, hence, we will only use the faster non-canonical variant in the remainder of this section.

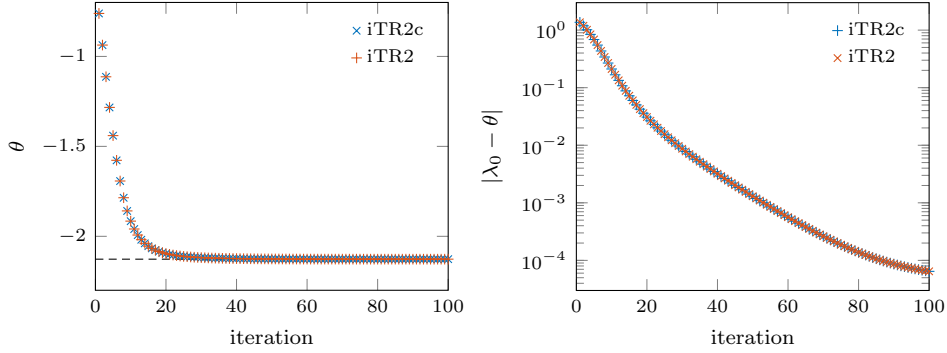
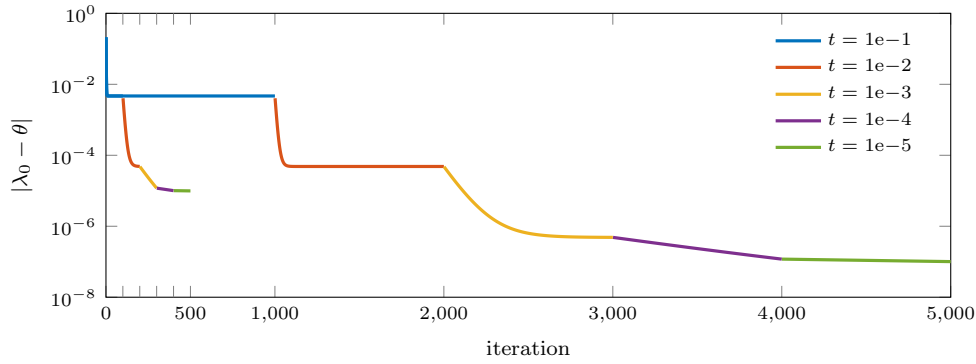
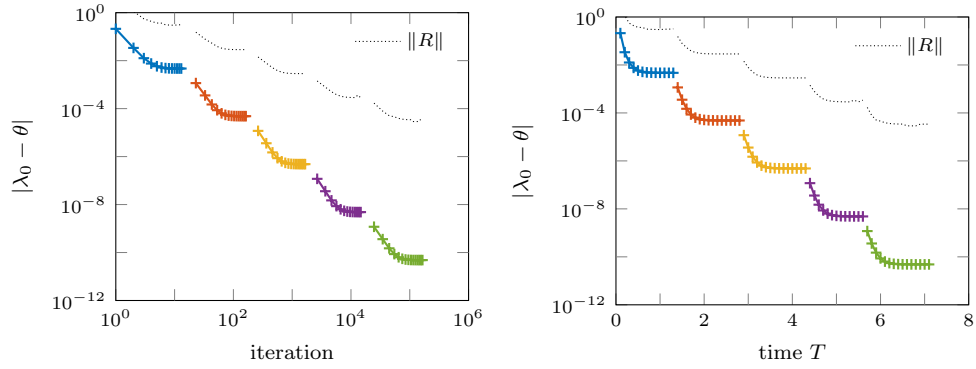
Next, we analyze the effect of the time step t on the convergence of Algorithm 3. Figure 5b depicts the convergence of 2 different runs where we respectively decreased the time step t after every 100 or 1000 iterations. Note that different time steps are indicated by different colors. From this figure it is clear that the time step control can have a significant effect on the overall attained accuracy. When t is decreased too soon, as in the first run, the power method tend to stagnate and further decreasing t does not help. On the other hand, we do not want to run too many iteration and therefore we will use the iTR residual, introduced in section 4.2, to detect stagnation.

As discussed in section 5.2, the total number of iterations can be reduced by gradually decreasing the time step t . Table 1 shows that running Algorithm 3 with a fixed time step $t = 1e-5$ requires at least twice the number of iterations and wall clock time than the adaptive time step approach, where t was divided by 10 when the first 3 digits of the residual norm $\|\text{Res}\|$ were not changing anymore in 3 consecutive convergence checks or in case the residual increased. The left plot in Figure 5c shows the corresponding convergence as a function of the iteration count. Note that by using the automatic time step adaption approach, the accuracy of the Ritz value is multiple orders of magnitude higher than achieved in both runs shown in Figure 5b. The right plot in Figure 5c shows the same results as the left one but in function of

TABLE 1

Wall clock times for one-dimensional transverse field Ising model with $g = 2$ and iTR rank $r = 10$.

t	iter	time [s]	iter	time [s]
1e-1			13	0.87
1e-2			150	0.72
1e-3			1,500	1.40
1e-4			13,000	4.80
1e-5	370,000	122.52	150,000	44.87
Total	370,000	122.52	164,663	52.67

(a) Comparison of the canonical and non-canonical variants of [Algorithm 3](#) for time step $t = 0.01$.(b) Influence of the time step t on the convergence of [Algorithm 3](#).(c) Convergence as a function of iteration count i and total time $T = \sum_i t_i$.FIG. 5. One-dimensional transverse field Ising model with $g = 2$ and iTR rank $r = 10$.

the total time $T = Nt$, with N the number of iterations of [Algorithm 3](#) for each t . Remark that the stagnation happens for every time step more or less at the same total time T , corresponding to roughly speaking the same power of $e^{-\mathbf{H}}$. We will use this observation in the next numerical experiments to change the frequency of the convergence check based on the current time step.

6.2. Spin $S = 1$ Heisenberg isotropic antiferromagnetic model. As a second example, we consider the isotropic antiferromagnetic case of the spin $S = 1$

Heisenberg model. The resulting Hamiltonian has the form of (1.3), with the following nearest neighbor interaction matrix

$$M_{k,k+1} = X_k \otimes X_{k+1} + Y_k \otimes Y_{k+1} + \Delta Z_k \otimes Z_{k+1},$$

where $\Delta = 1$, and X_k , Y_k , and Z_k the spin-1 generators of $SU(2)$

$$X_k = \frac{1}{\sqrt{2}} \begin{bmatrix} 0 & 1 & 0 \\ 1 & 0 & 1 \\ 0 & 1 & 0 \end{bmatrix}, \quad Y_k = \frac{1}{\sqrt{2}} \begin{bmatrix} 0 & -i & 0 \\ i & 0 & -i \\ 0 & i & 0 \end{bmatrix}, \quad Z_k = \begin{bmatrix} 1 & 0 & 0 \\ 0 & 0 & 0 \\ 0 & 0 & -1 \end{bmatrix}.$$

The smallest eigenvalue is $\lambda_0 \approx -1.4014840389712(2)$ [9].

Figures 6a to 6d show the convergence of Algorithm 3 for different iTR ranks $r = 10, 20, 30$, and 60 , respectively. For every case, we started with a time step $t = 0.1$ and the time step is divided by a factor of 10 whenever residual stagnation is detected with the criteria stated in the previous example. The frequency of the convergence check was set to $1/t$ in order to avoid computing too many (expensive) residual calculations. The corresponding wall clock time for the different runs are given in Table 2. This table illustrates again that the smaller the time step t the more iterations are required, hence, the larger the wall clock time.

When the rank of the iTR is too small, we see from Figure 6 that the Rayleigh quotient does not further improve even when the time step is reduced because the SVD truncation error is too large. On the other hand, we observe from Figures 6b to 6d that the residual norms in all these runs behave in a similar fashion. Since the iTR2 residual (4.24) is a projected residual, we cannot use it as the only metric for deciding when to terminate the power iteration. As illustrated in Figure 6e, the singular values given by the diagonal matrices of Definition 3.14 and in particular the smallest singular value together with the residual are good indicators for the actual accuracy of the approximate eigenpair of \mathbf{H} because the overall accuracy is bounded by both the Suzuki–Trotter splitting and SVD truncation error.

TABLE 2
Wall clock times corresponding to Figures 6a to 6d.

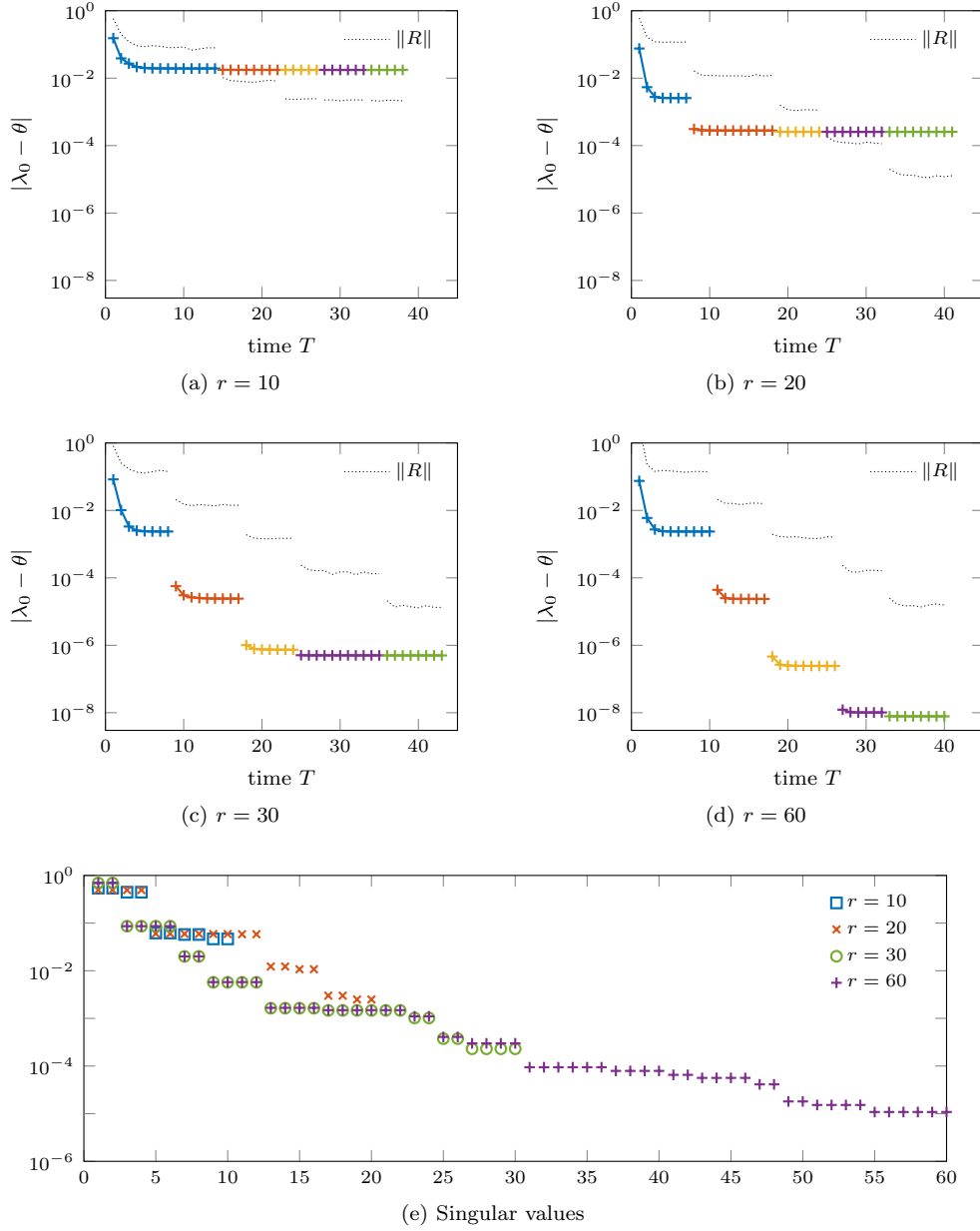
t	$r = 10$		$r = 20$		$r = 30$		$r = 60$	
	iter	time [s]	iter	time [s]	iter	time [s]	iter	time [s]
1e-1	140	0.60	70	0.71	80	1.04	100	3.83
1e-2	800	0.75	1,100	2.26	900	3.28	700	9.08
1e-3	5,000	3.27	6,000	8.63	7,000	19.60	9,000	96.78
1e-4	60,000	33.75	80,000	107.57	110,000	314.33	60,000	590.71
1e-5	500,000	288.10	900,000	1,190.97	800,000	2,137.29	800,000	7,521.75

6.3. Spin $S = 1/2$ Heisenberg model. As a last example, we consider the spin $S = 1/2$ Heisenberg model. The resulting Hamiltonian has the form of (1.3), with the following nearest neighbor interaction matrix

$$M_{k,k+1} = X_k \otimes X_{k+1} + Y_k \otimes Y_{k+1} + Z_k \otimes Z_{k+1},$$

where $X_k = \frac{1}{2}\sigma_x$, $Y_k = \frac{1}{2}\sigma_y$, $Z_k = \frac{1}{2}\sigma_z$, with $\sigma_x, \sigma_y, \sigma_z$ the Pauli matrices. The exact solution of the smallest eigenvalue is $\lambda_0 = -\ln(2) + \frac{1}{4} \approx -0.443147180559945$.

In Figure 7a, we plot the convergence history of the Rayleigh quotient θ to the exact eigenvalue λ_0 as well as the changes in the first (θ_1) and second (θ_2) terms of

FIG. 6. *Spin $S = 1$ Heisenberg isotropic antiferromagnetic model.*

(4.10) (excluding the $1/2$ factor) with respect to the total time T . In this calculation, we limit the rank of the iTR to 10 and used a fixed time step $t = 0.001$. As we can see, θ_1 approaches to λ_0 from above, but θ_2 can fall below λ_0 and eventually approaches λ_0 from below. Although θ_1 and θ_2 both converge towards λ_0 , the convergence is much slower than θ which is the average of θ_1 and θ_2 .

In addition to approximating the desired eigenvalue by the Rayleigh quotient, we can obtain another type of approximation by computing the eigenvalue of the

projected Hamiltonian matrix $H_{\neq 0}$ defined by (4.12). Because the summation in $H_{\neq 0}$ diverges, the eigenvalue of $H_{\neq 0}$ is not finite. However, the eigenvalue of the average of $H_{\neq 0}$ is finite and serves as an approximation to the average eigenvalue of \mathbf{H} defined in (1.3). To compute the average of $H_{\neq 0}$, we can first subtract θI from each of the terms $H_{-2-\ell}$ and $H_{1+\ell}$ in (4.13), for $\ell \geq 1$, where θ is the Rayleigh quotient. We then compute the geometric sums $H_L = H_{-2} + \sum_{\ell=1}^{\infty} (H_{-2-\ell} - \theta I)$ and $H_R = H_1 + \sum_{\ell=1}^{\infty} (H_{1+\ell} - \theta I)$, respectively, using the same techniques as discussed in the proof of Theorem 4.4 for the average residual calculation. We can show that both geometric sums converge. Next, we sum up H_L , H_{-1} , H_0 , and H_R after θI is subtracted from each of these terms. The subtraction of θI from H_L and H_R are made to account for the θI 's not subtracted from H_{-2} and H_1 , respectively, before the geometric sums were performed to yield H_L and H_R . After dividing the sum of all four terms by 4, we add θI back to form the total average of $H_{\neq 0}$, i.e.,

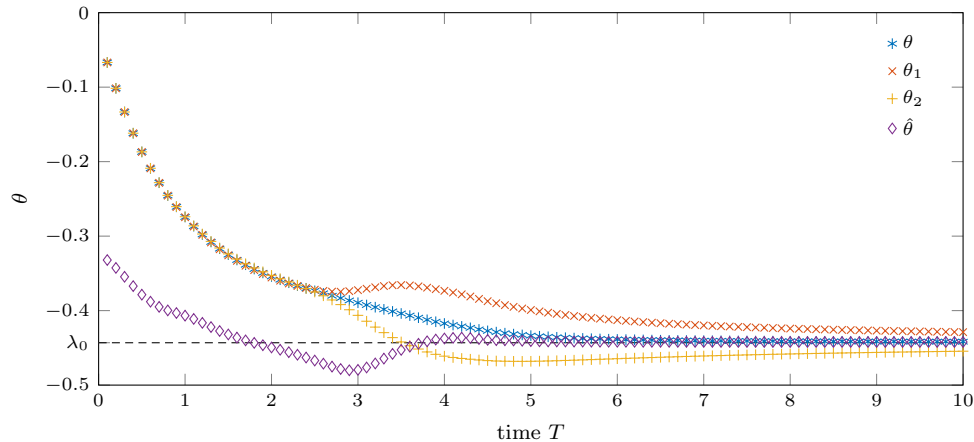
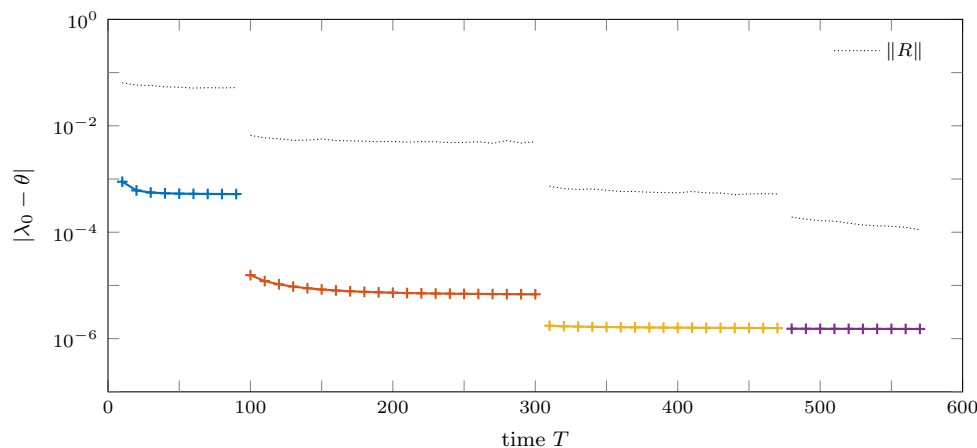
$$\hat{H}_{\neq 0} = (H_L + H_{-1} + H_0 + H_R - 4\theta I)/4 + \theta I = (H_L + H_{-1} + H_0 + H_R)/4.$$

In Figure 7a, the curve marked by the diamonds show that the eigenvalue $\hat{\theta}$ of the average $\hat{H}_{\neq 0}$ converges faster to λ_0 . However, computing the average $\hat{H}_{\neq 0}$ can be expensive when the rank of \mathbf{x} becomes large.

Figure 7b shows how the norm of the average residual and the difference between the approximate and exact eigenvalue change with respect to the total time T when the rank of the iTR is allowed to increased to 120. Even with this much larger rank, it is difficult to reduce the error in the approximate eigenvalue below 10^{-6} .

7. Conclusions. In this paper, we described a power method for solving a class of infinite-dimensional tensor eigenvalue problems for an infinite-dimensional matrix \mathbf{H} with a special type of Kronecker product structure, assuming that the approximate eigenvector can be represented by an infinite translational invariant tensor ring (iTR). We presented some algebraic properties of the iTR in terms of its transfer matrix and showed how to obtain a canonical form, which is convenient for manipulating an iTR in several calculations. We showed how the Rayleigh-quotient per site of an iTR \mathbf{x} with respect to the matrix \mathbf{H} can be efficiently computed. Although the power method itself is not new, the purpose of our paper is to clearly formulate this type of problem from a numerical linear algebra point of view and describe how a standard numerical algorithm such as the power method can be modified and applied to solve this type of problem. We have provided algorithmic and implementation details on how to carry out this procedure in a practical setting. In particular, we presented a better way to compute the Rayleigh quotient per site, and pointed out an alternative way to extract possibly better approximations to the desired eigenvalue. We also developed a practical and effective way to monitor the convergence of the power iteration by computing a projected residual estimate. Such a residual estimate is used to determine when to decrease the parameter t to improve convergence and when to terminate the power iteration.

We should note that the flexible power iteration is not the only method for solving this type of infinite-dimensional tensor eigenvalue problems. Alternative methods include the infinite density matrix renormalization (iDMRG) method and the variational uniform matrix product states (vUMPS) method. Due to the infinite dimensionality of the eigenvalue problem, special care must be exercised to compute quantities such as the Rayleigh quotient and the residual of an approximate eigenpair. We also need to take into account the approximation that must be made in the multiplication of the matrix exponential $e^{-\mathbf{H}t}$ with an iTR. A comparison to other algorithms and higher

(a) Convergence of the iTR Rayleigh quotient and its 2 comprising terms ($r = 10$ and $t = 0.001$).(b) Convergence as a function of total time for $r = 120$.FIG. 7. Spin $S = 1/2$ Heisenberg model.

order Lie–Trotter product formulas will be made in a future study.

REFERENCES

- [1] M. AIZENMAN AND B. NACHTERGAELE, *Geometric aspects of quantum spin states*, Comm. Math. Phys., 164 (1994), pp. 17–63, <https://doi.org/10.1007/BF02108805>.
- [2] M. T. BATCHELOR, *The Bethe ansatz after 75 years*, Phys. Today, 60 (2007), pp. 36–40, <https://doi.org/10.1063/1.2709557>.
- [3] H. BETHE, *Zur Theorie der Metalle*, Z. Phys., 71 (1931), pp. 205–226, <https://doi.org/10.1007/BF01341708>.
- [4] J. C. BONNER, H. W. J. BLÖTE, H. BECK, AND G. MÜLLER, *Quantum Spin Chains*, in Physics in One Dimension, J. Bernasconi and T. Schneider, eds., Berlin, Heidelberg, 1981, Springer Berlin Heidelberg, pp. 115–128.
- [5] M.-D. CHOI, *Completely positive linear maps on complex matrices*, Linear Algebra Appl., 10 (1975), pp. 285–290, [https://doi.org/10.1016/0024-3795\(75\)90075-0](https://doi.org/10.1016/0024-3795(75)90075-0).
- [6] S. V. DOLGOV, B. N. KHOROMSKIY, I. V. OSELEDETS, AND D. V. SAVOSTYANOV, *Computation of extreme eigenvalues in higher dimensions using block tensor train format*, Comput.

- Phys. Commun., 185 (2014), pp. 1207–1216, <https://doi.org/10.1016/j.cpc.2013.12.017>.
- [7] D. E. EVANS AND R. HØEGH-KROHN, *Spectral properties of positive maps on C^* -algebras*, J. Lond. Math. Soc., s2-17 (1978), pp. 345–355, <https://doi.org/https://doi.org/10.1112/jlms/s2-17.2.345>.
- [8] M. FANNES, B. NACHTERGAELE, AND R. F. WERNER, *Finitely correlated states on quantum spin chains*, Comm. Math. Phys., 144 (1992), pp. 443–490, <https://doi.org/cmp/1104249404>.
- [9] J. HAEGEMAN, J. I. CIRAC, T. J. OSBORNE, I. PIŽORN, H. VERSCHELDE, AND F. VERSTRAETE, *Time-dependent variational principle for quantum lattices*, Phys. Rev. Lett., 107 (2011), p. 070601, <https://doi.org/10.1103/PhysRevLett.107.070601>.
- [10] L. HULTHÉN, *Über das Austauschproblem eines Kristalles*, Ark. Mat. Astr. Fys., 26A (1938), pp. 1–106.
- [11] B. N. KHOROMSKIJ, *$O(\log N)$ -quantics approximation of N -d tensors in high-dimensional numerical modeling*, Constr. Approx., 34 (2011), pp. 257–280, <https://doi.org/10.1007/s00365-011-9131-1>.
- [12] D. KRESSNER, M. STEINLECHNER, AND A. USCHMAJEW, *Low-rank tensor methods with subspace correction for symmetric eigenvalue problems*, SIAM J. Sci. Comput., 36 (2014), pp. A2346–A2368, <https://doi.org/10.1137/130949919>.
- [13] O. MICKELIN AND S. KARAMAN, *On algorithms for and computing with the tensor ring decomposition*, Numer. Linear Algebra Appl., 27 (2020), p. e2289, <https://doi.org/10.1002/nla.2289>.
- [14] R. ORÚS AND G. VIDAL, *Infinite time-evolving block decimation algorithm beyond unitary evolution*, Phys. Rev. B, 78 (2008), p. 155117, <https://doi.org/10.1103/PhysRevB.78.155117>.
- [15] I. V. OSELEDETS, *Tensor-train decomposition*, SIAM J. Sci. Comput., 33 (2011), pp. 2295–2317, <https://doi.org/10.1137/090752286>.
- [16] R. PENROSE, *Applications of negative dimensional tensors*, in Combinatorial Mathematics and its Applications, D. J. A. Welsh, ed., vol. 1, New York, 1971, Academic Press, pp. 221–244.
- [17] D. PEREZ-GARCIA, F. VERSTRAETE, M. M. WOLF, AND J. I. CIRAC, *Matrix product state representations*, Quantum Inf. Comput., 7 (2007), pp. 401–430.
- [18] P. PFEUTY, *The one-dimensional Ising model with a transverse field*, Ann. Physics, 57 (1970), pp. 79–90, [https://doi.org/10.1016/0003-4916\(70\)90270-8](https://doi.org/10.1016/0003-4916(70)90270-8).
- [19] S. ROMMER AND S. ÖSTLUND, *Thermodynamic limit and matrix-product states*, in Density-Matrix Renormalization, I. Peschel, M. Kaulke, X. Wang, and K. Hallberg, eds., Springer Berlin Heidelberg, Berlin, Heidelberg, 1999, pp. 67–89, <https://doi.org/10.1007/BFb0106065>.
- [20] M. SANZ, *Tensor Networks in Condensed Matter*, PhD thesis, Technischen Universität München, 2011, <https://doi.org/10.14459/2011md1070963>.
- [21] G. VIDAL, *Classical simulation of infinite-size quantum lattice systems in one spatial dimension*, Phys. Rev. Lett., 98 (2007), p. 70201, <https://doi.org/10.1103/PhysRevLett.98.070201>.
- [22] S. R. WHITE, *Density matrix formulation for quantum renormalization groups*, Phys. Rev. Lett., 69 (1992), pp. 2863–2866, <https://doi.org/10.1103/PhysRevLett.69.2863>.
- [23] C. N. YANG AND C. P. YANG, *One-dimensional chain of anisotropic spin-spin interactions. II. Properties of the ground-state energy per lattice site for an infinite system*, Phys. Rev., 150 (1966), pp. 327–339, <https://doi.org/10.1103/PhysRev.150.327>.
- [24] V. ZAUNER-STAUER, L. VANDERSTRAETEN, M. T. FISHMAN, F. VERSTRAETE, AND J. HAEGEMAN, *Variational optimization algorithms for uniform matrix product states*, Phys. Rev. B, 97 (2018), p. 45145, <https://doi.org/10.1103/PhysRevB.97.045145>.
- [25] Q. ZHAO, G. ZHOU, S. XIE, L. ZHANG, AND A. CICHOCKI, *Tensor ring decomposition*, 2016, <https://arxiv.org/abs/1606.05535>. arXiv:1606.05535.